Flexibility in strategic flight planning

Bolic, T., Castelli, L., Corolli, L. and Scaini, G.

Flexibility in strategic flight planning

Abstract

A deterministic model that indicates flexibility of flights at the strategic level (up to 6 months ahead) taking into account changing airspace configurations and capacity is formulated. Flexibility is quantified by means of time windows (TWs). Flights complying with TWs guarantee that they will not impact negatively any other flight. Three variants of the model and three types of TWs are tested on a large-size data instance (the European network for an entire day of traffic). The model output specifies the constrained flights (i.e., with TWs shorter than the maximum size allowed for their definition), the constraining sector-hours and provides a list of saturated sector-hours. The meaning of each of the results is explored, across the three TW model variants, as well as the capability of the model variants to assure that capacity limits will not be exceeded. The criticality index, a measure of the sector-hour saturation, is introduced. This index can be used to identify areas for potential improvements. Sharing the information obtained from the TW model results at a strategic level can help both airlines and air navigation service providers (ANSPs) to improve the network status: airlines can decide to re-route heavily constrained flights (e.g., with one minute wide TWs), whereas ANSPs could decide to re-organise the capacity provision of the saturated airspace portions. The TW model can be re-run with the proposed changes, with the goal to assess the impact on both the individual stakeholders and the network. Thus, the model offers the measure of flight flexibility, and can be used as a tool to assess the impact of changes, helping in decision-making processes of airlines and ANSPs.

Keywords: flexibility, time windows, strategic flight planning, ATM, optimisation

1. Introduction

Before the unprecedented decrease due to the COVID-19 pandemic, air traffic in Europe had been growing from 2 to 4% a year since 2011. June 2019 saw the record number of daily flights (around 36 000 almost every day, with a maximum of more than 38 500 flights) handled by the European Air Traffic Management (ATM). Unfortunately, the amount of delay has been increasing as well, with the peak Air Traffic Flow Management (ATFM) delays in 2018 that were 61% higher than those in 2017 (Eurocontrol, 2019b). A significant portion of ATFM delay was accrued en-route, with en-route air traffic control (ATC) capacity (28%), weather (19%) and en-route ATC staffing (17%) being the major contributing causes. A part of the delay with ATC capacity and ATC staffing reasons is caused by less than perfect information exchange between the airspace users (flight demand) and the ATM capacity providers.

The European ATM system offers a high level of flight planning flexibility, as only the final flight plans need to be submitted, from 120 to 3 hours before departure (Network Manager, 2018). From conversations with different airline representatives we gathered that the earliest they tend to submit a flight plan is about 12 hours before the departure. On the one hand, this allows airspace users (AUs) the possibility to account for previously uncertain factors like weather forecasts, and thus create flight plans that are most convenient for the day of operations. On the other hand, this flexibility makes the ATM system less predictable, resulting in costs due to flow measures, and under-utilisation from a mismatch between available ATM capacity and traffic demand. When creating and subsequently submitting a flight plan AUs do not need to consider the capacity of ATM network elements involved, nor do they have that information. Thus, a precise traffic load on the airspace network is only known on the day of operations (i.e., in tactical phase). Conversely, the capacity provision (e.g., staffing levels) is usually planned about a year ahead and is updated as time progresses. On the day of operations, in cases when available airspace and airport capacity is lower than the planned air traffic, the Air Navigation Service Providers (ANSPs) and Network Manager agree on the ATFM measures to reduce the demand on the congested parts of the network. The ATFM measures impose delays on flights crossing congested network volumes. Alternatively, AUs have the option to re-route around the area in question to avoid

ATFM delay. These delays and deviations are very costly to airlines, e.g., estimated to be 1.93B € in 2018, and 1.76B€ in 2019 (Performance Review Commission, 2019).

Hence, capacity-demand imbalances, and consequent delays, are not only caused by unforeseen factors, like weather, but are also triggered by the lack of accurate information exchange at the required time horizons - months ahead for capacity provision planning, and hours ahead for flight (trajectory) planning - which often leads to congestion in parts of the network.

Congestion in the air transport network can have many causes, in both tactical and strategic settings, which can be tackled from different points of view, depending on the impacted stakeholders. Many such air transport problems can be solved using techniques from operations management (Koksalmis, 2019). They include, but are not limited to the following: demand and delay forecasting, delay reduction, crew and runway scheduling, and gate assignment. In demand forecasting, Meyn (2002) studied simple probabilistic methods for demand prediction on sectors and airport arrivals, and more recently, Kolidakis and Botzoris (2018) used artificial neural network architectures. Delay forecasting: Güvercin et al. (2020) addressed the problem of forecasting flight delays of an airport while Delgado et al. (2021) analysed the risk of accruing delay at specific network elements and its economic impact for airspace users. Delay reduction is often addressed by introducing buffer times: the larger they are, the easier it is to absorb and thus not propagate delay (see, e.g., Sanjeevi and Venkatachalam (2020); Brueckner et al. (2021), and Eufrásio et al. (2021)). Crew scheduling, relying on Barnhart et al. (2003) who illustrate the specifics of the airline crew scheduling problem, recently linked the impact of uncertain flight times on the robustness of the crew pairs decisions (Wen et al., 2020) or the impact of delays on the reliability of scheduled crew pairings (Sun et al., 2020). Runway scheduling is of importance as runway capacity is often the bottleneck in the air transport network (see Ikli et al. (2021) for an up-to-date review). Gate assignment is important for the efficiency of airport operations, ensuring that aircraft do not need to wait on the ramp or in the air (for an overview on the literature, see Bouras et al. (2014)).

Most of these papers propose deterministic models. However, uncertainty often plays important part in the mentioned problems. A review of stochastic modelling applications for solving different air traffic problems under uncertainty is available in Shone et al. (2021).

This paper addresses a specific air transport problem, usually referred to as airspace congestion and mitigation. An extensive body of literature exists in this area, mostly dealing with tactical problems (i.e., on the day of operations). Initially, most of these studies focused only on airport operations as those were the main bottlenecks. In this context, the works on the Ground Holding Problem (ground delays are assigned to flights at one or more airports in order to respect airport capacities) were born, starting with Odoni (1987)'s seminal paper and then continued considering a multi-airport setting (Vranas et al., 1994a,b) up to the present day where dynamic and stochastic approaches are introduced (Estes and Ball, 2020). Later, the possibility of introducing delays in the air, as well as airspace capacity, was added (Bertsimas and Stock Patterson, 1998, 2000), managing to simultaneously take into account various aspects such as ground-holding, re-routing, speed control, and airborne holding on a flight-by-flight basis (Bertsimas et al., 2011). These studies are also important for the European ATM system where large portions of the airspace, particularly in central-northern Europe, are subject to demand greater than their capacity. In fact, as highlighted by Lulli and Odoni (2007), the resolution of air traffic flow management issues in Europe can be very complex due to the traffic flow regulation rules when multiple limitations exist simultaneously, both in the air and on the ground. Hence, the need to study solutions that take into account the fairness with which delays are assigned (see, e.g., Barnhart et al., 2012). It is out of scope of this paper to provide an extensive literature review on the tactical flight planning, but it is worth mentioning that there are continuous improvements in this area through the development of increasingly sophisticated models, based on different techniques. See for example the recent contribution from Xu et al. (2020) who propose a complex four module framework to reduce airspace users delays, or Liu et al. (2019) using machine learning to analyse ground delay program actions, or Ding et al. (2018) studying the impacts of post-departure flight rerouting on arrival times, or Woo and Moon (2021) who analyse airlines' rescheduling actions when subject to a ground holding programme. Tactical flight planning is also expected to be enhanced thanks to the opportunities given by data availability and the capabilities provided by novel data-driven modelling techniques (see, e.g., Olive and Basora, 2020). Nowadays, availability of significant amounts of historic and real-time data in aviation are prompting the more ubiquitous use of data science and data analytics for a variety of applications as described by Chung et al. (2020). As data availability grows, different models for different time horizons in the planning process are being developed.

In the flight planning area, to avoid delays due to the information exchange gap, it would be beneficial for all the stakeholders to exploit the past and current information in the early, *strategic* planning stages. The term *strategic* used here refers to the period from six months to a few days before operations. A small number of studies deals with the strategic capacity-demand balancing, as opposed to the above cited tactical ones. Ivanov et al. (2019) propose re-design of ATM where the Network Manager would coordinate capacity and demand management decisions by "ordering" needed configurations from ANSPs and assigning delays or re-routes to flights. The aim of the coordination is to minimise total costs. The effects of a more robust capacity planning are further investigated by Starita et al. (2020) where traffic and capacity provision uncertainties are taken into to consideration. Differently, Bolić et al. (2017) develop an integer programming model for *strategic flight planning* that uses past and early-shared flight-route information to find the best distribution of the proposed (4D) flight trajectories that respect the nominal capacity[1] of the proposed network configurations[2]. They show that an alleviation of demand-capacity imbalances at the strategic planning level may lead to a reduction of the number of ATFM interventions on the day of operations, and the reduction of consequent delays. To the best of our knowledge, this is the first attempt at defining large-scale strategic traffic distribution by enforcing sector capacity constraints using an optimisation model on a realistic air traffic network (historic data are used for network and traffic description). We will refer to this model as Strategic Air Traffic Assignment (SATA) throughout this work.

The SATA model assigns the scheduled/planned departure time and route for each flight. Flight cancellations are not allowed, and speed control is not taken into consideration, as it would make little sense in the strategic phase. The maximum allowed *shift* (difference between SATA-assigned times and requested times) to earlier or later departure/arrival times is bounded. Furthermore, the changing airspace configurations throughout the day and associated capacities are taken into account. However, as the model is deterministic, the resulting 4D trajectories could be construed to mean that all the flights need to adhere exactly to the specified timing constraints, which would greatly reduce the current levels of AU flexibility.

This paper extends the work in Bolić et al. (2017) by proposing a model that quantifies flexibility for each flight trajectory. We term this flexibility measure *time windows* (TWs). Time windows are time intervals around each sequential *operation* (departure, arrival or entry into a sector) of a flight. As long as the flight operation is performed within the time window, the flight will not cause disturbances (i.e., delay) to any other flight in the system, at any time. If a flight has to be performed in a highly congested environment with a number of interdependent flights, a 'small' delay may cause a large downstream effect. It follows that such flights are constrained to operate closely to their assigned times, and we refer to them as *constrained*. On the contrary, a flight is *unconstrained* when operated in a non-congested area where the same amount of delay may not have any impact other than the delay on the flight itself. In other words, should an unconstrained flight depart 'slightly after' the assigned time, it will not cause disruptions in the system. Thus, the *duration* of a time window is a measure of the flexibility that can be granted to perform the flight operation: the longer the duration of the time window, the greater the flexibility, of course. Since constrained and unconstrained flights may coexist at the same time in the network, the duration of time windows may vary among flights.

The TW concept in the ATM context is not entirely new, but so far it only addresses the execution (while en-route) or tactical planning (on the day of operations) phases of a flight. In the the execution phase, Berechet et al. (2009) and Han et al. (2010) explore the TWs along the flight trajectory. Margellos and Lygeros (2013) use Monte Carlo simulations to assess the probability of flights meeting their TW constraints. More recently, Rodríguez-Sanz et al. (2019, 2020) analyse the duration of TWs as a function of distance from the origin, showing that precision deteriorates with the distance, forcing larger TWs further away from the origin. In the tactical phase, Castelli et al. (2011) propose a formulation to maximise the global duration of TWs over a small set of approximately 6 500 flights, 30 airports, 145 sectors and 50 time periods. Their experimental environment is artificial as both airspace configuration and traffic demand are randomly generated. Nevertheless, it provides a depiction of the flight flexibility measure in a tactical setting, a few hours before departure.

The contributions of this paper are extending two of the mentioned studies. Firstly, the tactical TW model proposed by Castelli et al. (2011) is generalised to a strategic context, to a very realistic

[1]Nominal capacity is the number of allowed aircraft entries into a sector, under nominal conditions, within the defined time horizon, usually an hour.

[2]Airspace configuration defines how the airspace of an area control center is organised. It can be divided in a different number of airspace volumes, depending on expected traffic.

characterisation of the European airspace, by considering the main features of the European capacity management (see Appendix A for a description). Secondly, computational experiments are run on real data (traffic, airspace configurations, etc.), and on much larger instances (around 30 000 flights, 230 airports, 1 500 sectors and 1 440 time periods), as described in Section 5.

The TW model uses as input the results of the SATA model (Bolić et al., 2017), characterising the flexibility of flight operations. The SATA model identifies deterministic times for each flight operation, without explicitly providing information on how much flexibility is left to perform such operations. The TW model allows answering the question: what is the exact time span within which an operator is expected to perform operations without causing disruptions to others? These time spans are the so-called time windows, and as such offer a measure of the robustness of the solutions of the SATA model. The wider the time windows, the more robust the operations. Contrarily, narrow time windows indicate a possibly unstable solution that may easily lead to disruptions when put into practice.

As the proposed model addresses strategic flight planning, the *main contribution* of this work is the model that identifies the flexibility and constraints in the network, across multiple stakeholders, in the *strategic* flight planning phase. Furthermore, it can be used in the what-if scenario testing in the decision-making processes of AUs and ANSPs. The model identifies constrained and unconstrained flights and the distribution of the expected congestion in space and time across Europe. Once the TWs are assigned to flights, it is possible to identify the elements of the planned network configuration (i.e., sectors or airports) that are going to be saturated. Thus, already at the strategic/pre-tactical level, an indication of the flexibility or constraints imposed on flights, and saturated network elements can be obtained. This information can then be shared with all the stakeholders, for example through the rolling Network Operations Plan (NOP[3]).

The results we describe here are encouraging and highlights the opportunity to further explore ATM strategic aspects in order to better manage the system on the day of operations. The remainder of this paper unfolds as follows. Section 2 further describes the concept of time windows, and Section 3 presents their mathematical definition and the formulation of an integer linear programming model with the objective of maximising TW duration, i.e., the flexibility that can be granted to flights. To better exploit capacity constraints, Section 4 presents two variants of the initial TW model. The application of these models is performed on a real data instance (Section 5) and the computational results are shown in Section 6. The robustness of the results is analysed in Section 7. Discussions, next steps and concluding remarks are given in Section 8.

2. Time windows

Currently, the scheduled departure and arrival times are the only portions of the flight plan that are planned strategically (i.e., they are published for each season, six months in advance). The schedules take into account the capacities of some airports (those that are slot controlled), and do not take into account the airspace capacity. However, in order to provide a strategic indication of the flight flexibility (TW duration) for a specific day, we need the (nominal) capacities of the network elements to be able to determine the departure and arrival times, and trajectories for that day. This is the result obtained from the SATA model (see Section 1) where departure times, subsequent sector entry times (i.e., the trajectory), and arrival times are determined with the aim of minimising the difference between what airlines ask for and what they can realistically obtain due to the presence of capacity constraints. We refer to departure, arrival, and sector entry times calculated by SATA as *assigned* departure, arrival, and sector entry times, respectively. We use these as input data into our model.

For each flight trajectory, a TW is introduced at the departure airport, at each sector entry and at the arrival airport and is characterised by the assigned time and duration. Perhaps the most intuitive way to define TWs is to extend them forward into the future from the corresponding assigned departure, arrival and sector entry times. However, as we operate in the strategic planning phase, (i.e., before actual flight schedules are published), departure and arrival times earlier or later than the assigned ones may be considered. For this reason, we also explore two other possibilities where TWs can be extended both backward and forward in time, with respect to the assigned time, and the extensions can be symmetric or asymmetric. Thus, we introduce three types of TWs (Figure 1):

[3]NOP is the tool managed by the Network Manager that collects and shares information from different stakeholders, regarding the demand and available capacity, to mention some of the information.

- *Forward TWs*, where TWs can be extended only forward with respect to the assigned time.
- *Symmetric TWs*, where TWs extend both backward and forward from the assigned time, for the same number of time periods.
- *Asymmetric TWs*, where TWs extend both backward and forward from the assigned time, with different number of time periods between backward and forward extensions.

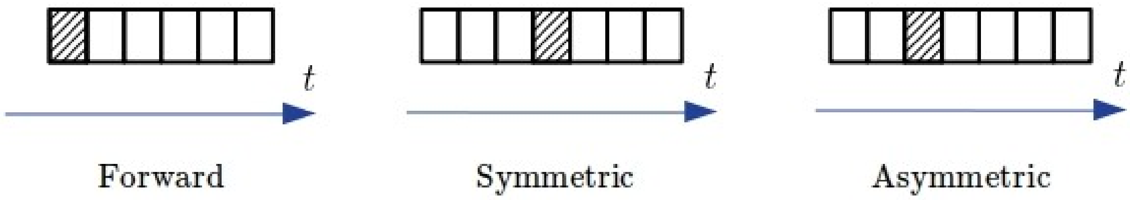

Figure 1: Three different types of TWs: Forward, Symmetric and Asymmetric. For each TW, the periods of time where the departure (or sector entry) can be executed are represented by white rectangles, while the assigned time is represented by a shaded rectangle.

3. Time window model formulation. The general case

The longer the duration of TWs, the greater the flexibility. Thus, the natural objective is to maximise the overall duration of all TWs. For this purpose, a binary linear programming model is formulated, to which we refer as the *TW model*. The formulation takes into account the following assumptions:

- The assigned times of all TWs are an input to the TW model. They are calculated by the SATA model, which - unlike most ATFM models (e.g., Bertsimas et al. (2011)) - takes into account the airspace configuration changes throughout the day, and multiple entries of a flight in any sector. TW assigned times and duration are computed separately because a formulation that simultaneously derives both turned out to be intractable, even in the simplest forward TW case (Corolli et al., 2010).
- Only one type of TWs is applied in any one run of the model.
- For a given flight, the duration of the TWs along the trajectory may vary depending on the area in which the flight is performed. For example, the departure airport could be in an area that is not very congested, but very crowded portions of airspace must be crossed during the flight. However, since the flexibility of a flight is limited by the TW of minimum duration, we impose that all TWs of a flight have the same duration, equal to the minimum one. Therefore, since all TWs are of the same duration and the flight speed is constant (see Section 1) once the departure TW of a flight has been determined, all the others are automatically identified. Different flights can have TWs of different duration, of course.
- The duration of a TW is measured in terms of *time periods*. For simplicity's sake, in this paper we always assume that a time period is equal to one minute. The generalisation to different time period sizes is straightforward.

We finally define as *sector-hour* a period of time (hour or less) in a day, linked with the specific portion of airspace (i.e., sector) or airport, having a defined capacity in that period of time. As airport capacities can be defined for arrival, departure or general (mix of arrival and departure) operations, for the sake of simplicity, we also refer to these airport-hour capacities as sector-hour capacities in the further text.

3.1. Notation

The notation used to define the TW models is the following:

3.1.1. Sets

$$\begin{aligned}
\mathcal{A} &\equiv \text{ set of airports, indexed by } a\\
\mathcal{S} &\equiv \text{ set of sectors, indexed by } s\\
\mathcal{F} &\equiv \text{ set of flights, indexed by } f\\
\mathcal{G} &\equiv \text{ set of pairs of flights } (f', f'') \text{ that are connected, with turnaround time } g_{f',f''}\\
\mathcal{R} &\equiv \text{ set of routes, indexed by } r \text{, where } r_f \text{ is the chosen route for flight } f\\
\mathcal{B} &\equiv \{dep, arr, gen, ent\} \equiv \text{ set of operations that can be performed by a flight,}\\
&\quad \text{where } arr, dep, \text{ and } gen \text{ stand for arrival, departure or generic movement type}\\
&\quad \text{(can be arrival or departure) at an airport, and } ent \text{ stands for entry into a sector}\\
\mathcal{C}_j^b &\equiv \text{ set of sector-hours linked with the operation } b \text{ at sector or airport } j \text{, indexed by } c\\
\mathcal{T}^c &\equiv \text{ set of time periods during which sector-hour } c \text{ is active}
\end{aligned}$$

3.1.2. Parameters

$$\begin{aligned}
orig_f &\equiv \text{ departure airport of flight } f\\
dest_f &\equiv \text{ destination airport of flight } f\\
n_f &\equiv \text{ number of elements (sectors and airports) along the chosen route } r_f\\
s_r^i &\equiv i\text{-th element of route } r\\
l_r^i &\equiv \text{ flight time from origin to the i-th element of route } r\\
d_f &\equiv \text{ assigned departure time of flight } f\\
g_{f',f''} &\equiv \text{ turnaround time between incoming flight f' and outgoing flight f'', performed by the same aircraft}\\
w_{max}^- &\equiv \text{ maximum number of time periods belonging to a TW preceding its assigned time}\\
w_{max}^+ &\equiv \text{ maximum number of time periods belonging to a TW subsequent or equal to its assigned time}\\
w_{max} &\equiv w_{max}^- + w_{max}^+ \equiv \text{ maximum duration of each TW}\\
w_{min} &\equiv \text{ minimum duration of each TW}\\
open_c &\equiv \text{ opening time period for sector-hour } c \text{ (i.e., opening time of sector-hour c)}\\
close_c &\equiv \text{ closing time period for sector-hour } c\\
\mathcal{Q}_c &\equiv \text{ capacity enforced during sector-hour } c\text{, (i.e., declared capacity of a sector } j\text{, during the sector-hour } c)
\end{aligned}$$

3.1.3. Parameter-depending sets

$$\begin{aligned}
\mathcal{T}_{f,i}^- &\equiv \text{ set of feasible time periods, previous to the assigned time } d_f + l_{r_f}^i,\\
&\quad \text{for flight } f \text{ to arrive at } i\text{-th element of its route } r_f\\
\mathcal{T}_{f,i}^+ &\equiv \text{ set of feasible time periods, subsequent or equal to the assigned time } d_f + l_{r_f}^i,\\
&\quad \text{for flight } f \text{ to arrive at } i\text{-th element of its route } r_f\\
\mathcal{T}_{f,i} &\equiv \mathcal{T}_{f,i}^- \cup \mathcal{T}_{f,i}^+ \equiv \text{ set of feasible time periods for flight } f \text{ to arrive at } i\text{-th element of its route } r_f
\end{aligned}$$

3.2. Decision variables

Decision variables are used to capture the duration of departure TW for each flight.

$$x_f(t) = \begin{cases} 1 & \text{if the TW for flight } f \text{ is open} \\ & \quad \text{for departure at time } t \\ 0 & \text{otherwise} \end{cases} \qquad \forall f \in \mathcal{F}, t \in \mathcal{T}_{f,1}$$

3.3. Objective function

The objective function maximises the total duration of all TWs.

$$max \sum_{f\in\mathcal{F},t\in\mathcal{T}_{f,1}} x_f(t)\cdot\gamma(t-d_f) \tag{1}$$

Weight coefficients γ ensure that TW duration is distributed as fairly as possible, i.e., the model will favour the assignment of TWs of similar duration to each of two flights, rather than the assignment of a large TW to one flight and a small one to another.

$$\gamma(\tau) = 1 - \frac{2|\tau|}{w_m\cdot|\mathcal{F}|} \qquad -w^-_{max} \le \tau \le w^+_{max}-1, w_m = max(w^-_{max}, w^+_{max}-1)$$

Coefficients $\gamma(\tau)$ are always non-negative. Since $|\tau| \le w_m$, it follows that $0 \le \frac{|\tau|}{w_m} \le 1$. Hence, $\gamma(\tau)$ is equal to 1 when $\tau = 0$ and decreases as $|\tau|$ grows. When $|\tau|$ is equal to w_m then $1 - \frac{2}{|\mathcal{F}|}$ is certainly non-negative for $|\mathcal{F}| > 1$ ($|\mathcal{F}| = 1$ is a trivial case that does not need to be investigated), hence:

$$0 \le 1 - \frac{2}{|\mathcal{F}|} \le \gamma(\tau) \le 1.$$

See Appendix B for a more detailed discussion on $\gamma(\tau)$ coefficients.

3.4. Constraints

3.4.1. Decision variable definition constraints

Binary decision variables $x_f(t)$ are monotone decreasing in $\mathcal{T}^+_{f,1}$: if a TW for flight f is open at time $t+1$ then it must also be open at time t.

$$x_f(t) \ge x_f(t+1) \qquad \forall f\in\mathcal{F}, t\in\mathcal{T}^+_{f,1} \tag{2}$$

$x_f(t)$ are monotone increasing variables in $\mathcal{T}^-_{f,1}$: if a TW for flight f is open at time $t-1$ then it must also be open at time t.

$$x_f(t) \ge x_f(t-1) \qquad \forall f\in\mathcal{F}, t\in\mathcal{T}^-_{f,1} \tag{3}$$

3.4.2. Time window duration constraints

There are two sets of TW duration constraints – minimum and maximum duration constraints. The minimum duration constraints guarantee that the specified minimum duration for TWs is respected.

$$\sum_{t\in\mathcal{T}_{f,1}} x_f(t) \ge w_{min} \qquad \forall f\in\mathcal{F} \tag{4}$$

The maximum duration constraints are simply respected by defining the $\mathcal{T}_{f,1}$ sets to contain a number of time periods equal to w_{max}.

$$\mathcal{T}_{f,1} \equiv \{d_f - w^-_{max}, \ldots, d_f, \ldots, d_f + w^+_{max} - 1\}$$

3.4.3. Connectivity constraints

Connectivity constraints guarantee that the time between the arrival of the incoming flight f' and the departure of the outgoing flight f'', performed by the same aircraft, is greater or equal to the turnaround time $g_{f',f''}$:

$$x_{f'}(t') + x_{f''}(t'') \le 1 \qquad \forall (f',f'')\in\mathcal{G}, t'\in\mathcal{T}_{f',1}, t''\in T_{f'',1}: t' + l^{n_{f'}}_{r_{f'}} + g_{f',f''} \ge t'' \tag{5}$$

3.4.4. Symmetry constraints

These constraints are used for the symmetric TW case only. They guarantee that the departure TWs are symmetrical (see Section 2) with respect to the period of time d_f in which the departure/entry is assigned, i.e., a TW is open for departure at time $d_f+\tau$ if and only if it is open at time $d_f-\tau$.

$$x_f(d_f+\tau) = x_f(d_f-\tau) \qquad \forall f\in\mathcal{F}, 1\le\tau\le w^+_{max}-1 \tag{6}$$

3.4.5. Capacity constraints

Capacity constraints ensure that sector and airport capacities are respected for all sector-hours. The SATA is a deterministic model, and it allocates trajectories with the precision of one minute. If the SATA trajectories are flown within one minute accuracy, we can be sure that all the sector-hour capacities in the network, both saturated and unsaturated ones, are respected. However, the improvement we want to bring with the TW model is to determine how much flexibility in terms of time can be given to each trajectory. To be able to optimally compute the TWs, we need to take into account the possibility that TWs can extend into adjacent sector-hours, as shown in Figure 2.

As TWs can extend backward and forward with respect to the assigned time of entry into a sector-hour, in Figure 2 we depict three possible cases of positioning of TWs within a sector-hour, for three flights having assigned entry times: after the closing of sector-hour c (flight f_1), within the sector-hour c (flight f_2), and before opening of sector-hour (flight f_3). For these three flights, $d_f + l^i_{r_f}$ is the time period in which this, i-th operation, is assigned, and is represented by the shaded rectangles in the figure. $\mathcal{T}^-_{f,i}$ is the set of time periods within which the sector entry can be performed earlier than scheduled, and $\mathcal{T}^+_{f,i}$ is the set of time periods in which the sector entry can be on time (i.e., shaded rectangle) or postponed. The orange rectangles show the time periods t in which the three flights may reserve the unit of capacity in this particular sector-hour c. As can be seen, the TW of the flight f_3 crosses into the sector-hour c from the previous sector-hour, the TW of the flight f_2 is in its entirety within the sector-hour, and the TW of the flight f_1 crosses back into the sector-hour c from the subsequent sector-hour c_{+1}. However, it can happen that this particular sector-hour is not the most constraining one along the trajectory. In case another sector-hour is more constraining, it might happen that the TW cannot be extended to the orange coloured time periods.

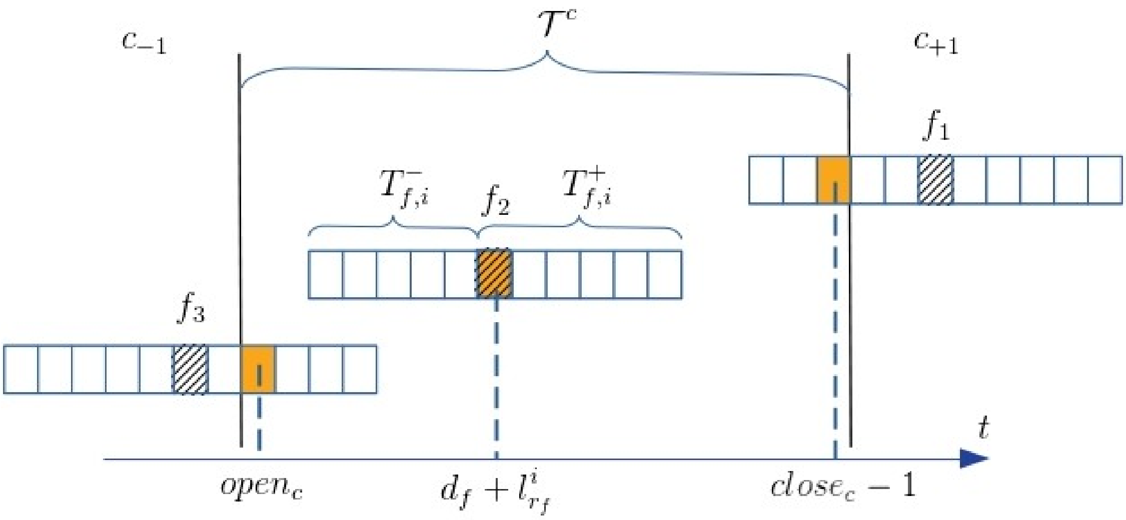

Figure 2: Description of time periods in which the unit of capacity may be reserved in sector-hour c, for 3 different flights crossing the sector-hour c, open and active in time periods $t \in \mathcal{T}^c$.

With this in mind, the number of departures dep^a_c and arrivals arr^a_c at an airport a during the sector-hour c, are calculated as follows:

$$dep^a_c := \sum_{\substack{f\in\mathcal{F},t\in\mathcal{T}^c\cap\mathcal{T}_{f,1}:\\ v^{1,dep}_{f,c}(t)\wedge orig_f=a}} x_f(t) \tag{7}$$

$$arr^a_c := \sum_{\substack{f\in\mathcal{F},t\in\mathcal{T}^c\cap\mathcal{T}_{f,n_f}:\\ v^{n_f,arr}_{f,c}(t)\wedge dest_f=a}} x_f(t-l^{n_f}_{r_f}) \tag{8}$$

Further, the number of entries ent^j_c in the sector-hour c, of a sector j is calculated as follows:

$$ent_c^j := \sum_{\substack{f\in\mathcal{F}, i\in[2,n_f-1], t\in\mathcal{T}^c\cap\mathcal{T}_{f,i}: \\ v_{f,c}^{i,ent}(t)\wedge s_{r_f}^i=j}} x_f(t - l_{r_f}^i), \tag{9}$$

In all equations (7)-(9), $v_{f,c}^{i,b}(t)$ is a logical parameter that determines whether the time period t is the first period, closest to $d_f + l_{r_f}^i$, in which flight f may reserve capacity in sector-hour $c \in \mathcal{C}_{s_{r_f}^i}^b$. Since TWs can extend backward as well as forward with respect to the assigned time b (i.e., entry into a sector along the trajectory), $v_{f,c}^{i,b}(t)$ is defined as:

$$v_{f,c}^{i,b}(t) := (t \in \mathcal{T}^c \cap \mathcal{T}_{f,i}^{+} \wedge (t = d_f + l_{r_f}^i \vee t = open_c)) \vee (t \in \mathcal{T}_{f,i}^{-} \cap \{close_c - 1\})$$

By exploiting the monotony of the decision variables as defined by constraints (2) and (3), if the time window for the i-th operation b of flight f is open at time t such that $v_{f,c}^{i,b}(t) = true$, then the flight reserves a unit of capacity in sector-hour c, otherwise it does not. For instance, $v_{f,c}^{i,b}(t) = true$ for each of the orange coloured time-periods shown in Figure 2.

Thus, the capacity constraints can be expressed as:

$$dep_c^a \leq \mathcal{Q}_c \qquad \forall a \in \mathcal{A}, c \in \mathcal{C}_a^{dep} \tag{10}$$

$$arr_c^a \leq \mathcal{Q}_c \qquad \forall a \in \mathcal{A}, c \in \mathcal{C}_a^{arr} \tag{11}$$

$$dep_c^a + arr_c^a \leq \mathcal{Q}_c \qquad \forall a \in \mathcal{A}, c \in \mathcal{C}_a^{gen} \tag{12}$$

$$ent_c^j \leq \mathcal{Q}_c \qquad \forall j \in \mathcal{S}, c \in \mathcal{C}_j^{ent} \tag{13}$$

Constraints (10) impose the departure capacity at the airport (if defined), constraints (11) the arrival, and constraints (12) the general airport capacity. Constraints (13) impose sector capacity.

4. Variants of TW model

The mathematical model described in the previous Section 3 could lead to overly conservative solutions because it may reserve an excessive amount of capacity for each flight: in case a TW extends over two sector-hours (see Figure 2), the model reserves a whole unit of capacity in either of the two sector-hours, even though the flight will use only one unit of capacity. Thus, we term this initial variant as the *conservative* TW model. To allow for less conservative solutions, two variants of the conservative TW model are introduced, based on Castelli et al. (2011):

- *proportional TW model*,
- *intermediate TW model*.

To define these variants, capacity counts (7), (8) and (9) are modified through the introduction of a *capacity utilisation coefficient* $\beta_{f,c}^i(t)$ ($\in [0,1]$). The coefficient $\beta_{f,c}^i(t)$ assigns to each period t of the i-th TW assigned to flight f the fraction of unit of capacity to be reserved in sector-hour c. Thus the capacity counts are modified to:

$$dep_c^a := \sum_{\substack{f\in\mathcal{F}, t\in\mathcal{T}^c\cap\mathcal{T}_{f,1}: \\ orig_f=a}} \beta_{f,c}^1(t) \cdot x_f(t) \tag{14}$$

$$arr_c^a := \sum_{\substack{f\in\mathcal{F}, t\in\mathcal{T}^c\cap\mathcal{T}_{f,n_f}: \\ dest_f=a}} \beta_{f,c}^{n_f}(t) \cdot x_f(t - l_{r_f}^{n_f}) \tag{15}$$

$$ent_c^j := \sum_{\substack{f\in\mathcal{F}, i\in[2,n_f-1], t\in\mathcal{T}^c\cap\mathcal{T}_{f,i}: \\ s_{r_f}^i=j}} \beta_{f,c}^i(t) \cdot x_f(t - l_{r_f}^i) \tag{16}$$

4.1. Proportional TW model

In the *proportional TW model*, for a TW assigned to a flight f that extends across the sector-hour c, only a fraction of unit of capacity of c equal to the fraction of time periods of the TW present in sector-hour c is reserved.

That is, if there is a 9-period TW, where the first 6 periods are located within sector-hour c_1 and the remaining 3 periods extend into the sector-hour c_2, as shown in Figure 3, only $\frac{2}{3}$ of the unit of capacity of c_1 and $\frac{1}{3}$ of the unit capacity of c_2 will be reserved. In the case of sector-hour c_1, this is expressed by the ratio:

$$\frac{\sum_{t\in\mathcal{T}^{c_1}\cap\mathcal{T}_{f,i}} x_f(t-l^i_{r_f})}{\sum_{t\in\mathcal{T}_{f,i}} x_f(t-l^i_{r_f})} = \frac{2}{3} \qquad \forall f\in\mathcal{F}, i\in[1,n_f], c\in\mathcal{C}^b_j : s^i_{r_f}=j \tag{17}$$

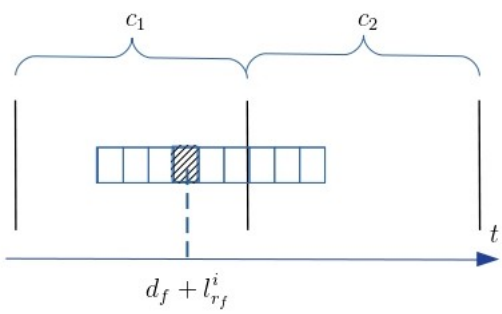

Figure 3: Example of a 9-period TW, with the 6 periods lying within sector-hour c_1 and the remaining 3 periods extending into c_2.

Since the share of capacity to be reserved in a sector-hour c is given by the sum of the contributions of all the time periods during which c is active and the TW is open, the capacity utilisation coefficients $\beta^i_{f,c}(t)$ for the *proportional TW model* need to be defined in such a way that:

$$\sum_{t\in\mathcal{T}^{c}\cap\mathcal{T}_{f,i}} \beta^i_{f,c}(t) = \frac{\sum_{t\in\mathcal{T}^{c}\cap\mathcal{T}_{f,i}} x_f(t-l^i_{r_f})}{\sum_{t\in\mathcal{T}_{f,i}} x_f(t-l^i_{r_f})} \qquad \forall f\in\mathcal{F}, i\in[1,n_f], c\in\mathcal{C}^b_j : s^i_{r_f}=j \tag{18}$$

4.2. Intermediate TW model

Further, in the *intermediate TW model*, if the sector-hour c contains $d_f + l^i_{r_f}$, i.e., the assigned time of arrival of flight f at the i-th element of its route r_f, one unit of capacity of c is reserved (as in the *conservative model*). In case the sector-hour c does not contain the period of assigned arrival, a fraction of unit of capacity of c, equal to the fraction of the number of TW periods lying within c is reserved (as in the *proportional model*).

Taking up the previous example shown in Figure 3, if there is a 9-period TW, where the first 6 periods, including $d_f + l^i_{r_f}$, are within sector-hour c_1, and the other 3 periods extend to sector-hour c_2, one unit of capacity of c_1 and only $\frac{1}{3}$ of the capacity of c_2 will be reserved.

Thus, for the *intermediate model*, capacity utilisation coefficients $\beta^i_{f,c}(t)$ are defined in such a way that:

$$\sum_{t\in\mathcal{T}^{c}\cap\mathcal{T}_{f,i}} \beta^i_{f,c}(t) = \begin{cases} 1 & \text{if } d_f + l^i_{r_f} \in \mathcal{T}^c \\ \frac{\sum_{t\in\mathcal{T}^{c}\cap\mathcal{T}_{f,i}} x_f(t-l^i_{r_f})}{\sum_{t\in\mathcal{T}_{f,i}} x_f(t-l^i_{r_f})} & \text{otherwise} \end{cases} \qquad \forall f\in\mathcal{F}, i\in[1,n_f], c\in\mathcal{C}^b_j : s^i_{r_f}=j$$

The details on the implementation of these coefficients are given in Appendix C, from which we also understand that they cannot be computed for asymmetric TWs in the intermediate and proportional variants. Table 1 summarises TW model variants and TW types under analysis in this paper.

Table 1: Summary of TW model variants and TW types under study.

	TW model variants						
	Conservative			**Intermediate**		**Proportional**	
TW type	Forward	Asymmetric	Symmetric	Forward	Symmetric	Forward	Symmetric

5. Data instance

TW models are tested on a day of real air traffic data, encompassing the entire European Civil Aviation Conference (ECAC) airspace. Different data items are needed to run the models, including flights, airspace configuration, capacities of resources (sectors and airports), and trajectories. The SATA model also requires aircraft types and their operational costs, fuel costs, route charges (unit rates), and airline cost profiles. The data on air traffic and air network structures are sourced from EUROCONTROL's Demand Data Repository 2 (DDR2). Cost data are taken from the report by Cook and Tanner (2015).

The data instance is created with the traffic from September 1st, 2017, a busy, but not unduly disrupted day. This day is ranked as the fifth busiest day in 2017, but with significantly lower ATFM delay with respect to the better ranked days in 2017.

5.1. Flights

On September 1st, 2017, 36 881 flights were counted. However, we exclude the military flights, overflights, helicopters, and flights departing from and arriving at the same airport, thus ending with 29 917 flights. Flight data consists of flight IDs, origin, destination, aircraft type, and requested departure times, all of which is sourced from DDR2 last-filed flight plans (so called *m1* data).

5.2. Airspace configuration and capacity of resources

Each Area Control Center (ACC) usually changes the configuration of the active sectors several times throughout the day, to best accommodate the changing traffic demand (both number of flights and flow directions). The TW models apply changing sector configurations, the ones in place in Europe on September 1st 2017, which counted 204 airports and 1 458 sectors (this is the total number of different sectors that were open at some point on the chosen day, they are not all open/active at the same time). The capacity of active sectors is also needed, in order to define the capacity constraints. We sourced the airport and sector nominal capacities from the DDR2 data.

5.3. Routes and departure times

For each Origin-Destination (OD) – aircraft type combination we determine a set of routes to be used by the SATA model. The routes are sourced from the two AIRAC cycles in 2017 - February (AIRAC 1702) and September (AIRAC 1709). However, to reduce the number of routes, we consider only the ones that differ significantly from one another in terms of geographical distance (more than 30 kilometres where the distance between the two routes is maximal). The SATA model takes as an input these sets of routes, and requested departure times from m0 (initial flight plan) where available, or m1 (last filed flight plan) files, and allows for a plus/minus 30 minute shift around those times. The SATA results, which are departure, subsequent sector entry, and arrival times (based on a route chosen by the optimisation) are then used as input in the TW model.

6. Experimental results

After running the SATA model to allocate trajectories and departure, sector entry and arrival times to all flights, we ran the different TW models to determine the flexibility that can be granted to each flight. All experiments were performed using the FICO XPRESS optimization software, version 8.8.0. It is a software specifically devoted to solving mixed-integer linear programming problems. We ran it on a 64 bit Intel(R) Xeon(R) W-2145 @3.70GHz 16 core CPU computer, having 32GB of RAM memory and Debian 18.04 operating system. The computational time for the SATA model was 260 seconds. Computational times for all TW model variants are reported in Table 2. The conservative TW model is the fastest, as it is also the simplest (in terms of number of feasible solutions), with the proportional model being the slowest: after 300 seconds the forward case exhibits a relative gap equal to 3.86% (fifth row of Table 2), meaning that if we consider as optimal the best solution obtained so far (370 951 minutes, fourth row of Table 2), we make an error which is at most equal to 3.86%, i.e., optimal solution $\leq$ 1.0386∗(best solution). In absolute terms, this means that the optimal solution could be at most 14 910 minutes higher than the best solution (last row of Table 2). As we are considering 29 917 flights, it follows that, on average, a TW could not be more than half a minute larger (14 910/29 917 = 0.498). Since the proportional forward case provides the highest objective function value among all TW model variants and types (see again the fourth row of Table 2), by stopping after 300 seconds we only provide a tiny underestimate of the maximum possible flexibility. In all other cases the optimality gap is even lower: 1.22% for the proportional symmetric case, 0.02% in the intermediate forward case, and 0% otherwise.

Table 2: Run times, objective function values, and optimality gaps of TW model variants for different TW types (w_{max} = 15 min).

	Conservative			**Intermediate**		**Proportional**	
TW type	Forward	Asymmetric	Symmetric	Forward	Symmetric	Forward	Symmetric
Run time (sec.)	2.2	2.2	3.2	300	300	300	300
Best Solution (min.)	339 950	368 589	315 010	345 488	325 558	370 951	335 386
Relative gap (%)	0.00	0.00	0.00	0.02	0.00	3.86	1.22
Absolute gap (min.)	0	0	0	78	6	14 910	4 140

For better clarity in the presentation of the results, here we define the term *constrained flight* in a formal manner. A constrained flight f has a TW, with the duration w^f that is shorter than the maximum w_{max}. In other words, unconstrained flights are all the flights with TW duration equal to w_{max}.

In this section, we first present the analysis of the duration of the TWs in different TW model variants and across various TW types (Section 6.1). Then, in Section 6.2 we evaluate the impact that the use of the intermediate and proportional variants has on capacity constraints compliance, as the model formulation does not ensure it (see details in Section 4).

6.1. Flexibility across TW model variants

Figure 4 shows the share of constrained and unconstrained flights across the three TW model variants ($w_{max} = 15 min$). As expected, the number of constrained flights per TW model variant is inversely proportional to the level of capacity utilisation and therefore the conservative method has a greater number of constrained flights than the intermediate method, which in turn has a greater number than the proportional one.

Also the type of TW, namely forward, symmetric and asymmetric, has an impact on the number of constrained flights. In all the three TW model variants, forward TWs always produce the lowest number of constrained flights when compared with asymmetric (only conservative TW model) and symmetric TW type. Again, it is expected, as forward TWs extend only in one direction, while the other two TW types can reach limits in both forward and backward directions.

	Conservative			**Intermediate**		**Proportional**	
TW duration	**Forward**	**Asymmetric**	**Symmetric**	**Forward**	**Symmetric**	**Forward**	**Symmetric**
1	3 166	205	6 005	3 185	5 849	2 337	5 471
2	735	272	0	728	0	527	0
3	730	280	1 204	711	1 090	472	868
4	731	295	0	683	0	507	0
5	787	368	1 225	730	1 032	531	832
6	674	2 551	0	619	0	508	0
7	616	728	1 088	553	879	478	691
8	732	756	0	634	0	495	0
9	639	734	1 178	557	904	446	727
10	739	2 793	0	600	0	499	0
11	667	1 102	1 239	512	970	477	818
12	607	1 084	0	458	0	442	0
13	707	1 142	1 122	537	785	480	801
14	700	1 082	0	592	0	452	0
15	17 687	16 525	16 856	18 818	18 408	21 266	19 709

Table 3: Distribution of flights across TW duration.

Table 3 shows the distribution of flights across TW durations, with w_{max} = 15 min.

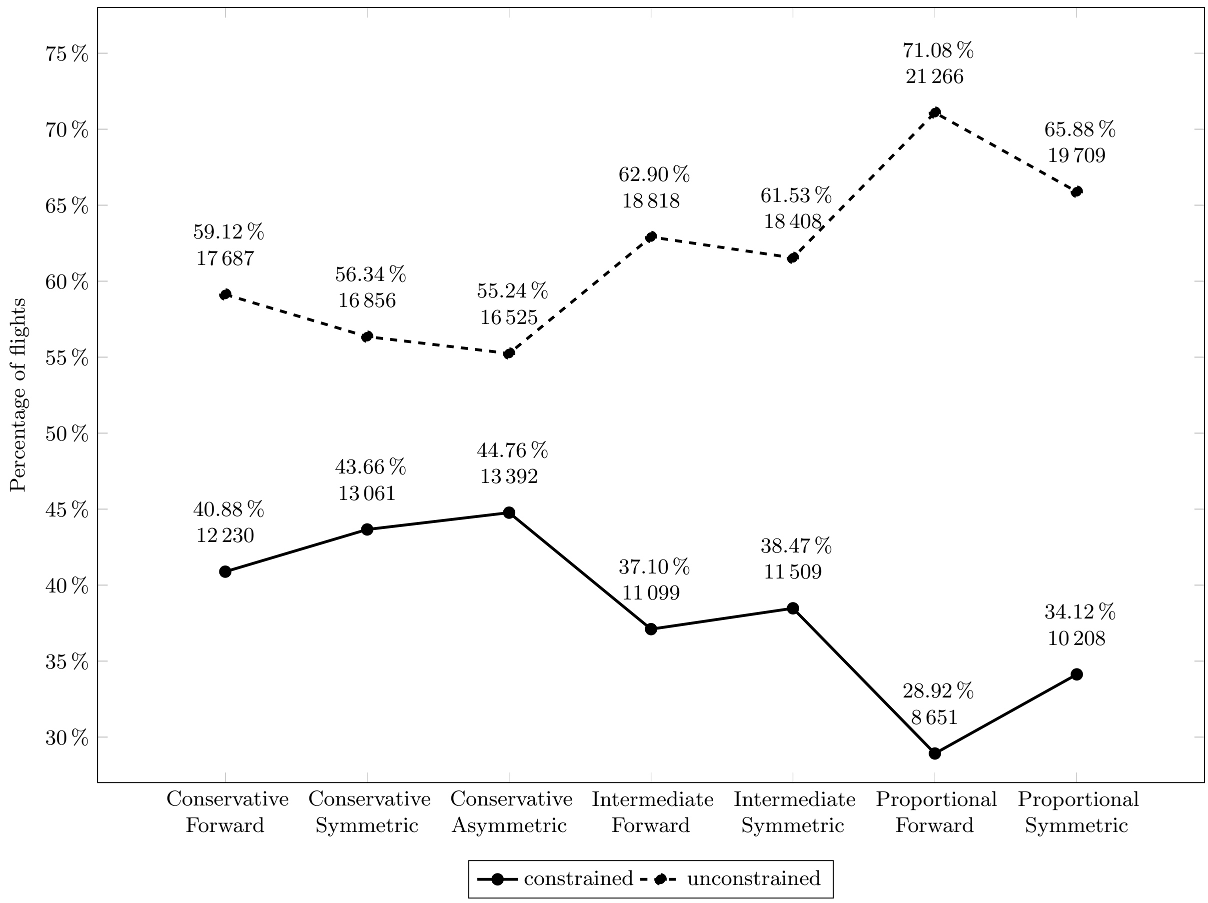

Figure 4: Number and percentage of constrained and unconstrained flights across TW model variants per TW type.

- Forward TWs. About a quarter of all the constrained flights have very tight constraints (1 min), while the rest are distributed across longer TW duration. From the operational point of view, a flight with 1 min TW means that it has to be performed with extreme precision - arriving at all scheduled points along the trajectory within a minute of the assigned time.

- Symmetric TWs. The TW duration is always an odd number as each TW is being extended for one additional minute both forward and backward. Here, between 30 and 40% of all constrained flights have a TW of only one minute. Hence, there are many more severely constrained flights than in the forward TW case. Once again, the conservative model has the most constrained flights across all TW durations, followed by the intermediate and then proportional model.

- Asymmetric TWs. A different behaviour is experienced in this case, which involves the conservative TW model only, as shown in column "Asymmetric" that illustrates the situation where TWs can extend from 5 minutes before to 10 minutes after the assigned time. The distribution of the TW duration is different with respect to the forward and symmetrical cases. First, this is the case that provides the lowest number of unconstrained flights (last row). In addition, we see that the largest share of constrained flights have TWs of 10 minutes, followed by TWs of 6 minutes. Instead, the number of extremely constrained flights (i.e., TWs of 1 minute) is very low, the lowest among all the different TW models and type variants presented here. Thus, the asymmetric TW type on one hand produces the highest number of constrained flights. On the other hand, it gives higher flexibility to constrained flights.

The very different distribution of constrained flights in the Asymmetric type when compared with the Symmetric and Forward ones is due to the applied constraints. Asymmetric, Forward and Symmetric types require increasingly stringent constraints to allow a longer TW. Take for example a flight f, with departure time at 10:00 from a_1 airport, and the trajectory that requires entry into sector s_1 at 10:10, in sector s_2 at 10:30 and landing at airport a_2 at 10:55. To assign a 2-minute Asymmetric TW to f it is necessary that all the airports and sectors along the trajectory have sufficient capacity to allow entry 1 minute before, or 1 minute after the assigned time of entry. In this case we would have two possibilities:

- TW sequence 1: a_1 = [10:00,10:01], s_1 = [10:10,10:11], s_2 = [10:30,10:31], a_2 = [10:55,10:56]
- TW sequence 2: a_1 = [9:59,10:00], s_1 = [10:09,10:10], s_2 = [10:29,10:30], a_2 = [10:54,10:55]

For a 2-minute Forward TW it is necessary that a_1, s_1, s_2 and a_2 have sufficient capacity to allow entry 1 minute *after* the assigned time, which is the first of the two possibilities in the Asymmetric type case. Finally, for a 2-minutes Symmetric TW it is necessary that a_1, s_1, s_2 and a_2 have sufficient capacity to allow entry both 1 minute before, and 1 minute after the assigned time. Thus, it requires both Asymmetric type case alternatives to be met, to then assign a 3-minute TW.

These examples help us understand the existence of two peaks in the distribution of constrained TWs, and its relation with the other two TW types. The first, the 6-minute TWs category represents the flights for which it is not possible to postpone the departure with respect to the assigned time. However, they could depart up to 5 minutes earlier. These flights would be assigned a 1-minute Forward TW, as the earlier start is not a possibility here. Also in a Symmetric type case, only 1-minute TW would be assigned as the symmetric extension backward and forward is not possible. The second peak represents flights having 10-minute TWs, for which earlier start is not possible, but that can depart up to 10 minutes later. These flights would have been assigned a 1-minute Symmetric TW and a 10-minute Forward TW or longer.

To sum up, there are clear differences between the three TW model variants, with the proportional model being the one that identifies the lowest number of constrained flights. However, this is offset by the large proportion of constrained flights having the most constrained TWs - almost half of all constrained flights are assigned 1 minute TW. The conservative TW model, with the Asymmetric TW type offers the highest flexibility (in terms of longer TWs) to the constrained flights. As such, we choose this particular model variant to further explore the impact the change of various parameters may have on the number of constrained/unconstrained flights, as shown in Section 7.

6.2. Capacity violations analysis

As already mentioned, the SATA model always respects capacity constraints. Therefore in each TW model variant and type, capacity constraints are not violated as long as all flights are executed at their assigned times. If, on the other hand, an operation is executed within a TW but at a time period other than the assigned one, the proportional and intermediate approaches may not guarantee that the capacity is respected. Thus, we have to verify whether and to what extent the use of the two model variants lead to capacity breaches.

The capacity utilisation across sector-hours for both intermediate and proportional models is simulated by assigning a random departure time for each flight, within its associated TW. Based on these new departure times, subsequent sector entry times (and arrival at the destination airport) along the trajectory are calculated. The new entry times are used to compute the capacity utilisation counts for all sector-hours. The capacity utilisation is then compared with nominal sector-hour capacities.

Departure times are randomised using the following three probability distribution functions:

- *Uniform*: all time periods within a TW can be chosen for departure with equal probability.
- *Triangular-like*:
  - Forward TWs: the probability monotonically decreases with time and hence the first time period has the highest probability for departure and the last time period the lowest.
  - Symmetric TWs: the probability monotonically decreases with time, symmetrically backward and forward. Thus, the assigned time period has the highest probability for departure, while the first and the last time periods have the lowest probability.
- *Mixed*: the SATA-assigned time period has 0.5 probability to be chosen, whereas all the other time periods equally share the remaining probability.

Table 4: Percentage of sector-hours for which the capacity is violated. Values averaged over 100 000 random instances (w_{max} = 15min).

	Intermediate model			Proportional model		
TWs	Uniform	Triangular	Mixed	Uniform	Triangular	Mixed
Forward	0.12	0.05	0.06	1.71	1.36	1.57
Symmetric	0.05	0.03	0.02	0.31	0.25	0.26

We ran 100 000 simulations for each combination of the TW model (intermediate and proportional), probability distribution (uniform, triangular-like, mixed), and TW type (symmetric and forward). Each simulation was run for 29 917 flights, over 24 008 sector-hours.

Table 4 shows the percentage of sector-hours for which the capacity is violated. These values are the average values across 100 000 simulations. Just for illustration, in case of the intermediate TW variant, forward TW type, and uniform distribution, about 29 sector-hours (0.12% out of 24 008 sector-hours) have their capacity violated. We observe that when the uniform distribution is applied slightly higher numbers of capacity violations occur with respect to the triangular-like and mixed distribution cases. In terms of absolute numbers of excess flights, our results show that on average, across 100 000 runs:

- Intermediate TW model: from 1.0 to 1.1 excess flights;
- Proportional TW model: from 1.1 to 1.4 excess flights.

For further illustration, the maximum number of flights exceeding sector-hour capacity across all the simulations is 11, which only occurs in one sector-hour in Italy from 13:00 to 14:00. For example, the sector depicted in Figure 5 is one of those for which the capacity was breached by 11 flights (sector-hour capacity is 76). The inspection of the actual entry count data (i.e., what actually happened on the day) shows a few cases of exceeding the capacity for 11 or 13 flights across several sector-hours. Further, we looked at entry counts across more days, and found out that the count is often higher than nominal capacity, going up to 100 flights an hour. This leads us to conclude that the maximum capacity breaches unearthed in the simulations fall under the regular operations.

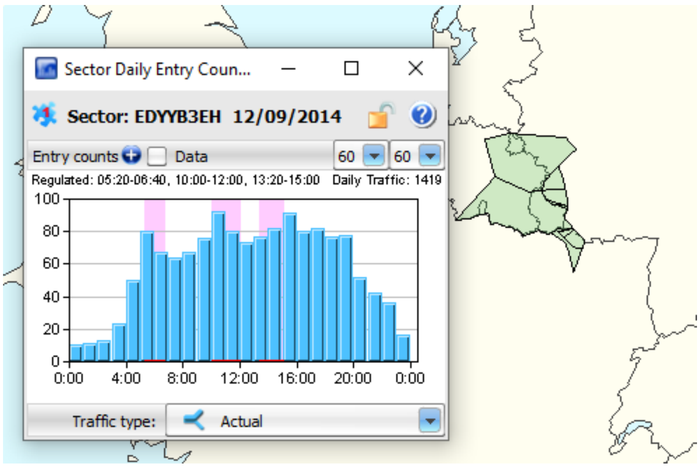

Figure 5: Sector that had a few significant capacity violations in the simulations for feasibility testing.

From the results presented in the Table 4, the intermediate TW model presents a significantly lower number of capacity violations than the proportional one, and the symmetric TW type results in fewer capacity violations. Thus, we conclude that both the proportional and intermediate ways of assigning capacity are feasible, as they result in a very low number of capacity violations, and the magnitude of violations is usually handled in the daily operations.

7. Robustness analysis

In this section, we vary some key input parameters and analyse the effects of the variations on the number of constrained/unconstrained flights, i.e. on flight flexibility. First, we consider the variation of minimum or maximum TW duration (Section 7.1). Next, we study the modification of capacity, where we first define the *saturated* sector-hours and then analyse the impact the variation of their capacity has on flights (Section 7.2). Finally, we assume that some flights do not respect their TWs, where their actual departure time ends-up being outside the assigned (departure) TW (Section 7.3). As mentioned at the end of Section 6.1, we use the conservative TW model, with the Asymmetric TW type for all the analyses, with all TWs ranging from -5 to +10 minutes from the assigned time.

7.1. Variation of the minimum and maximum TW duration

The first analysis involves the variation of the minimum TW duration, that can be changed from 1, over 3 to 5 minutes. As can be seen in Figure 6, the minimum TW duration variation impacts the result very little, by slightly diminishing the number of constrained flights only when minimum TW is set to be 5 minutes. The second parameter we analyse is the maximum TW duration, looking at 15 and 20 minute variations. We take only these two values into account as smaller value, like 10 minutes, is generally considered to be too short. Similarly, the TWs longer than 20 minutes make little sense, as an average flight time in Europe is between 90 and 120 minutes. The change of maximum TW duration from 15 to 20 minutes results in the much higher number of constrained flights (Fig. 7). This is due to the fact that the capacity needs to be reserved for a longer period of time.

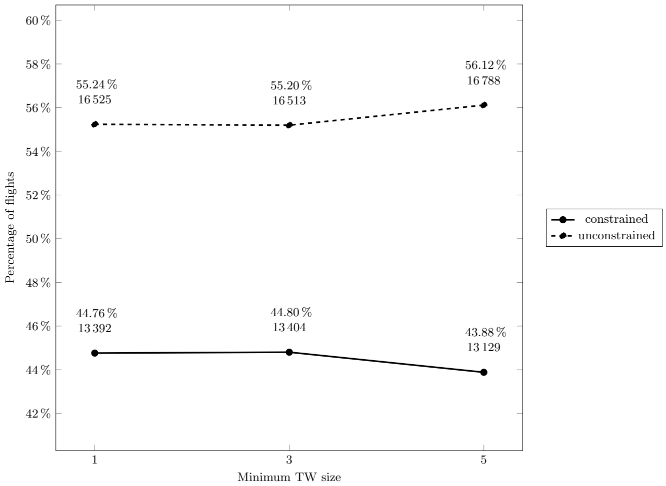

Figure 6: Constrained vs. unconstrained flights for different values of minimum TW duration - 1, 3, 5 min

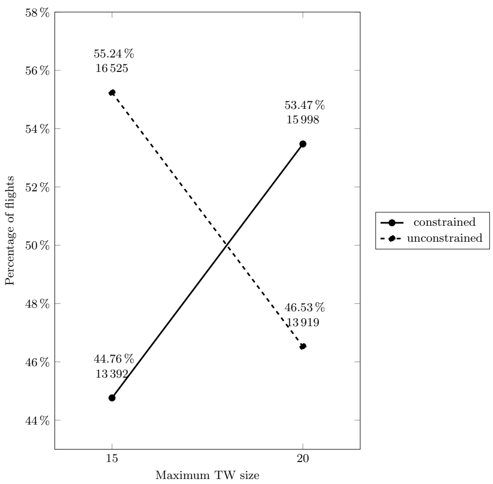

Figure 7: Constrained vs. unconstrained flights for different values of maximum TW duration - 15 or 20 min

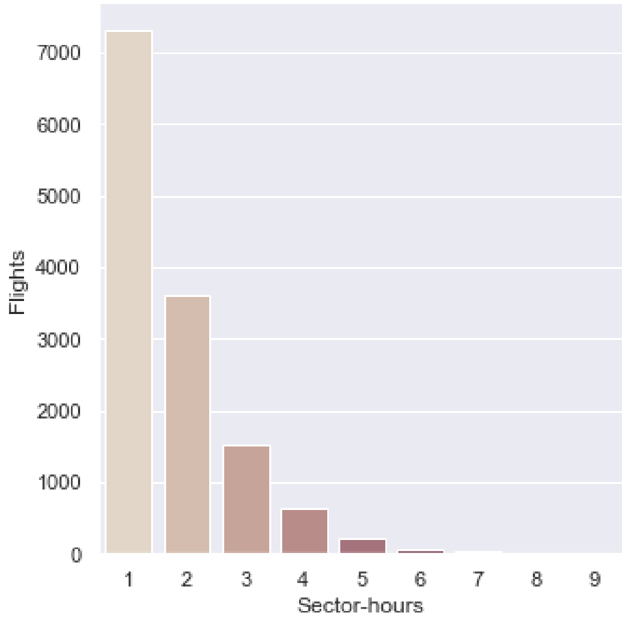

Figure 8: Flights constrained by number of sector-hours.

7.2. Constrained flights and saturated sector-hours

Even though both intermediate and proportional TW models reserve the capacity in a less constraining manner than the conservative model, they both have a great number of very constrained flights, for both forward and symmetrical TW type (see Section 6.1). In order to avoid having a great number of very constrained flights, in the following analysis we will focus on the conservative TW model, with the asymmetric TW type, $w_{max} = 15$ min with $(-5, 10)$ maximum backward and forward extension, respectively.

Once it is ascertained that there are constrained flights, the natural next step is to find the sector-hours constraining the traversing flights. We term these sector-hours *saturated*.

Definition. A *saturated sector-hour* is a sector-hour where the TW duration of some (constrained) flights cannot be equal to the maximum allowed value w_{max} because the capacity limit is reached.

The saturated sector-hours indicate the bottlenecks in the network, and limit the flight flexibility. The flight flexibility could be improved by increasing the capacity of saturated sectors-hours, if and where possible. To be able to choose where it is best to intervene, we introduce a criticality index, defined as follows:

Definition. The Criticality index k_c measures the degree of criticality of a sector-hour as the total additional number of time periods that all flights constrained by the same sector-hour would have if it had sufficient capacity. The criticality index k_c is:

$$k_c = \sum_{f \in F^c} (w_{max} - w^f),$$

where F^c is the set of constrained flights that have TW duration constrained by the used-up capacity of the saturated sector-hour c. A high criticality index denotes the sector-hour for which a rise in capacity would bring the greatest increase of the objective function value. On the whole, the criticality index of a sector-hour is overestimating the criticality as a constrained flight could be limited by multiple sector-hours (see Figure 8).

Figure 9 shows trajectories constrained by the sector shaded white, at flight level 340, at 10:15. The saturated sectors are coloured from red to white, depending on the criticality index value. The most constrained trajectories are shown in light yellow that turns to dark with more flexibility (i.e., longer TW duration). A flight from EDDS (Stuttgart, Germany) to GCLP (Gran Canaria, Spain) is shown, which is constrained by this sector, and has a TW of 10 minutes, only going forward without the possibility of anticipating the assigned time.

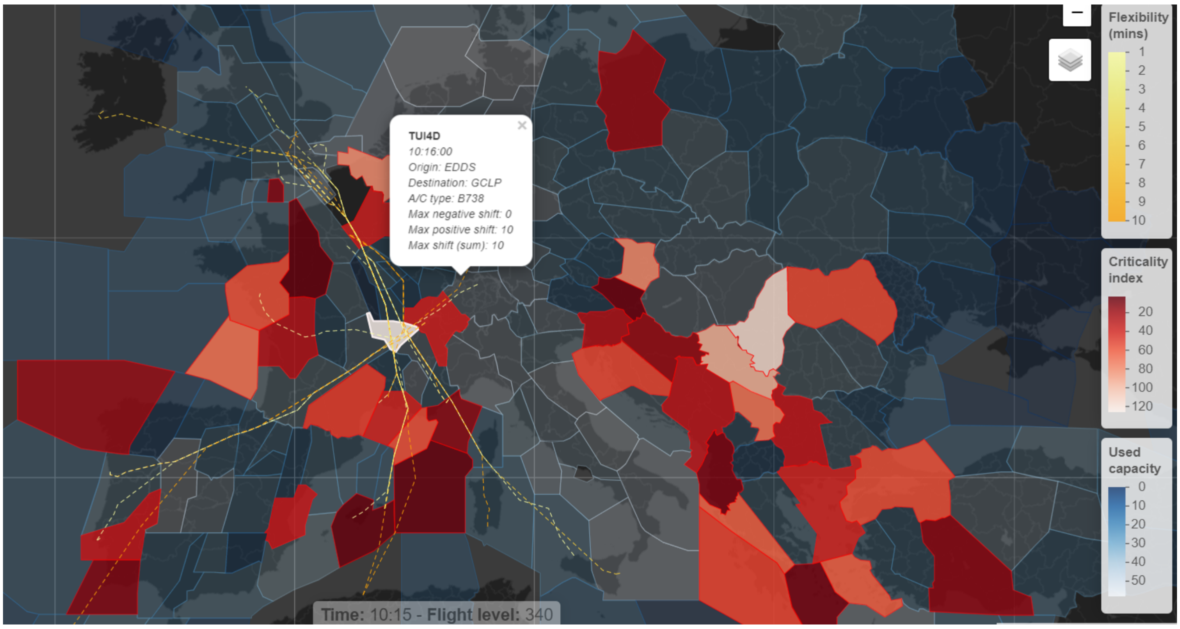

Figure 9: Examples of constrained flights and saturated sector-hours (source: ADAPT visualisation tool https://visualization.adapt-h2020.eu/).

Table 5 shows the five sector-hours with highest criticality indices, out of 2 310 saturated sector-hours identified by the model. The start time, end time, capacity, number of constrained flights, and criticality index are shown for the chosen sector-hours. As can be seen, these constrain a significant number of flights, when compared to their respective capacity.

Table 5: Criticality index for a sample of sector-hours (conservative TW model, asymmetric TWs (-5, 10), $w_{max} = 15$.)

Sector	Start time	End time	Capacity	Constrained flights	Criticality index
LTAAIE	21:00	22:00	47	53	429
EGTTEAST	21:00	22:00	40	49	388
EGTTSOUTH	21:00	22:00	70	55	354
LTBAALL	05:00	06:00	86	44	347
EGTTNWD	07:00	08:00	60	45	344

Thanks to this indicator it is possible to identify the sector-hours for which an increase in capacity brings the greatest benefits in terms of flexibility. In fact, Figure 10 shows how the total TW duration (the objective function of the conservative, asymmetric (-5,10) TW model) varies when the capacity of the sectors is increased by 5%. The increase is applied on different groups of sectors. We start with the 10% of the least saturated sector-hours (criticality index from 1 to 9), continue on the second 10% (criticality index from to 9 to 15) and so on. It is shown that by increasing the capacity by 5% on only the 10% of the sector-hours with the highest criticality index (141-429), a non-negligible increase (from the initial objective function value of 368 589 to 372 566, +1.08%) in the duration of the TWs, therefore in flexibility, is obtained. In fact, in terms of flights this means that 2 041 flights could increase the duration of their TWs with an overall gain of 3 977 minutes and 280 more unconstrained flights (+1.7%). This could be very useful information for the ANSPs and Network Manager as they could identify in advance the portions of the airspace where it would be most beneficial to intervene to ensure greater flexibility to flights on the day of operations.

7.3. TW violation analysis

The TWs are determined in a strategic setting, not taking into account many sources of tactical uncertainties. As such, in the tactical setting, TW violations may occur for a variety of factors, such as

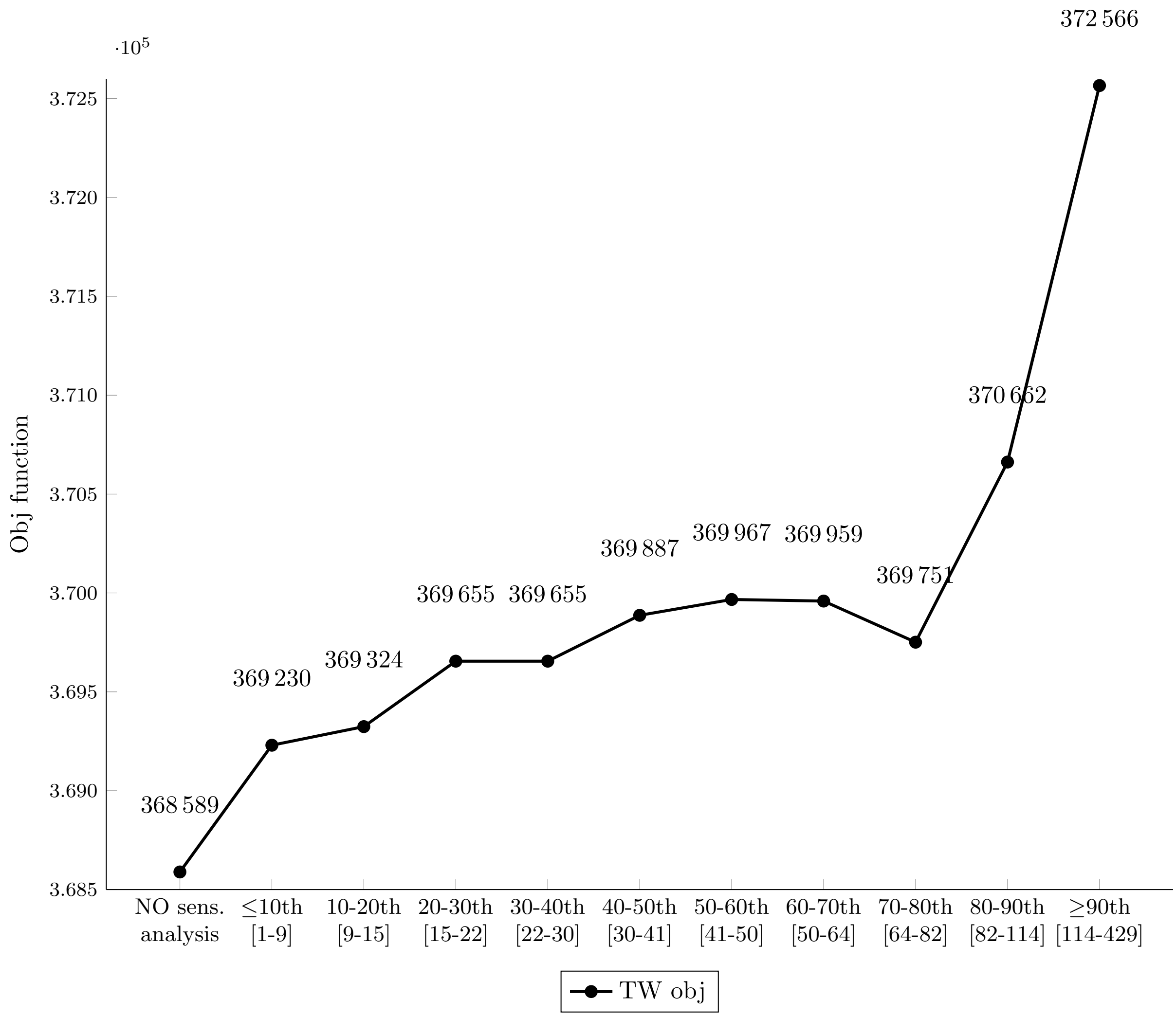

Figure 10: TW objective function value variation when the capacity is increased by 5% for the saturated sector-hours.

weather conditions, or reactionary delays due to crew or aircraft rotations, or other disruptions. These inconveniences may lead to the situation where the assigned TWs are too narrow, and thus difficult to be respected by airlines. For this reason, the robustness of the TW model needs to be checked against TW violations, evaluating what happens when a number of flights is not able to meet them, and thus need to be assigned new, previously unassigned resources. As an example, let the assigned time of a flight f be equal to 10:00, with the departure TW from 09:55 to 10:10. On the day of operations, however, flight f is only able to depart at 10:15, i.e., 5 minutes after the end of its TW. The problem to be faced is: when can this flight be rescheduled? Can the airline expect to find available resources at 10:15, or will the flight incur additional delay?

To answer these questions, we simulate the tactical delays and analyse their impact on the flight flexibility. To do so, we apply the probability distribution of real departure delays at all European airports in September 2017 as illustrated in Figure 11a (Mitici et al., 2019). The distribution takes into account all the delays caused by airline and airport processes, and all ATFM delays. However, this exact amount of delays would be overly pessimistic in our setting, since the TW model allows for better strategic planning. As such, departure times and TWs respect airspace capacities which can reduce ATFM delays due to capacity and staffing reasons (see Bolić et al. (2017)). Thus, we want to study cases in which airlines are not able to meet TWs due to factors other than those addressed in the strategic planning. To do so, we adjust this delay distribution in two ways. First, from Figure 11a we observe that there is a share of flights that actually depart before their scheduled time. Since flights that are ready ahead of their assigned time represent non critical situations (e.g., night or early morning flights), we constrain

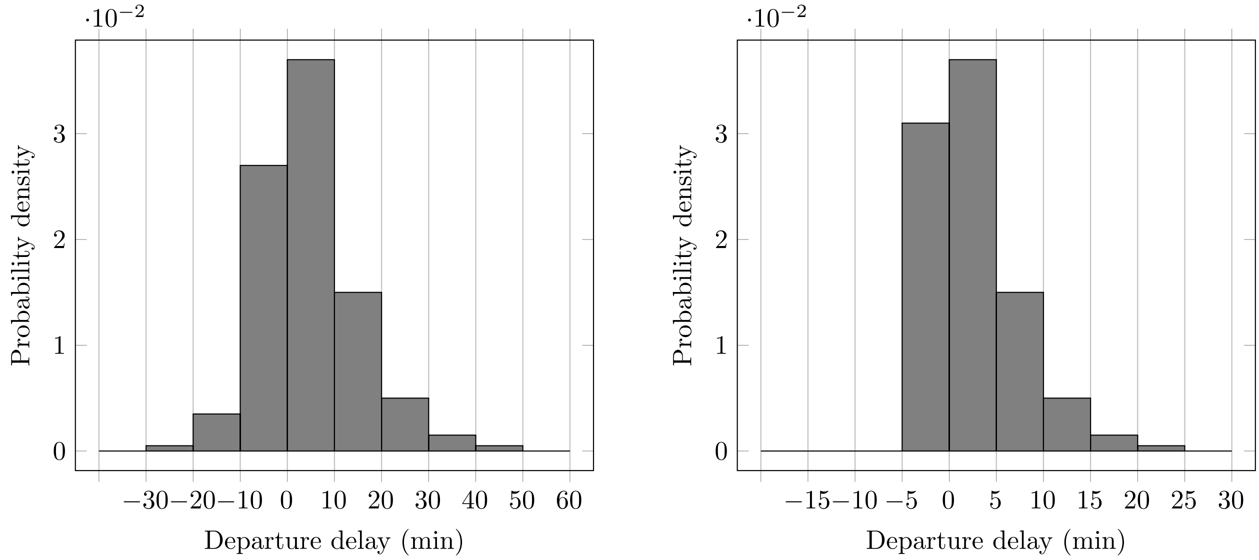

(a) Original distribution.

(b) Re-scaled distribution, factor of 0.5.

Figure 11: Distribution of departure delays at all European airports in September 2017.

the delay distribution to the −5 minutes (start time of the TW) on the left side. Second, to account for lower ATFM delays due to strategic planning, we re-scale the original probability distribution by a multiplicative factor of 0.25, 0.5 and 0.75. For example, with a re-scaling factor of 0.5, a delay of 10 minutes is re-scaled to $10 * 0.5 = 5$ minutes (Figure 11b).

Let $\mathcal{D} \subseteq \mathcal{F}$ be the subset of flights that are expected to depart after the end of their departure TW according to these distributions. On average $\mathcal{D}$ is composed of 6.0% of the total number of flights for a re-scaling factor of 0.25, 14.5% for 0.5, and 22.9% for 0.75, respectively. A flight $f \in \mathcal{D}$ is referred to as *delayed* flight and d_f^D is the *delayed* departure time as assigned by the delay distribution. Since d_f^D is outside the departure TW for all $f \in \mathcal{D}$, there is no guarantee that it is possible to respect network capacities for all flights $f \in \mathcal{F}$, and there might be the need to further delay some of these flights (either in $\mathcal{D}$ and/or in $\mathcal{F} \setminus \mathcal{D}$) to accommodate them. For each flight $f \in \mathcal{F}$, we also define as *TW violation* the difference between its departure time and the end of its departure TW. By setting the limit to 60 minutes after the end of the departure TW, updated departure times d_f^U to minimise TW violations, while respecting the nominal capacities of the network, are computed by means of a new TW robustness optimisation model (its mathematical formulation is available in Appendix D). All delayed flights must be assigned an updated departure time equal to or later than the delayed one, i.e., $d_f^U \geq d_f^D \; \forall f \in \mathcal{D}$.

Number of flights	**Rescaling factor**		
	0.25	**0.5**	**0.75**
TW violation > 0 min	3 886 (13.0%)	7 000 (23.4%)	9 543 (31.9%)
TW violation > 10 min	348 (1.2%)	986 (3.3%)	2 150 (7.2%)
TW violation > 20 min	146 (0.5%)	329 (1.1%)	579 (1.9%)
TW violation > 30 min	66 (0.2%)	159 (0.5%)	243 (0.8%)
TW violation > 40 min	31 (0.1%)	80 (0.3%)	116 (0.4%)
TW violation > 50 min	15 (0.1%)	43 (0.1%)	63 (0.2%)
Average TW violation (min)	4.2	5.9	7.3

Table 6: Distribution of delayed flights and average TW violation per delayed flight, averaged across 100 runs for 3 different rescaling factors. The percentage values refer to the total number of flights (29 917).

Table 6 shows the results of the TW robustness model. From the first row, we see that to accommodate all delayed flights, the number of flights violating their TWs slightly increases (from 6.0% to 13.0% for the 0.25 re-scaling factor, from 14.5% to 23.4% for 0.5, and from 22.9% to 31.9% for 0.75, respectively). It means that some flights in $\mathcal{F} \setminus \mathcal{D}$ also have to depart after the end of their TWs. However, we notice that for all three re-scaling factors most flights violate their TWs for less than 10 minutes, and even in the worst scenario (re-scaling factor = 0.75) the share of flights that need to depart more than 20 minutes after the end of their departure TW sharply drops to less than 2%. In real operations, the average delay per delayed flight was reported to be 28.4 minutes in 2019 (Eurocontrol, 2019a). Considering that the average TW violation per delayed flight (last row of Table 6) with re-scaling factor = 0.75 is just 7.3 minutes, which may be on top of at most 10 minutes of TW width after the assigned time, for a total of 17.3 minutes, the average delay per delayed flight is much lower than in current, mostly tactical operations. Further, the limited percentage of flights with larger violation values indicates that the tail of violations distribution is limited, having little impact on major disruptive events. Thus, we believe that the TWs proposed in this paper are a robust tool that may be used in operational strategic flight planning.

8. Discussion and concluding remarks

8.1. Discussion of strategic flight planning implications

The current European ATM system offers great flight planning flexibility, which is very tactical. Moving towards a more strategic way of planning will be acceptable as long as a viable compromise between flexibility and predictability can be achieved. The time windows (TW) models presented here demonstrate that it is possible to assign a measure of flexibility, i.e., a TW, to each flight and identify saturated elements of the network. As the model is computationally fast, it could be used to first assign flexibility and detect the network bottlenecks. As a second step, it could be used in the what-if scenarios aimed at improving the overall stakeholder and network situation. Here we discuss shortly two possible examples - change of airspace configuration or flight re-routes.

The saturated sector-hours identify where and when the ATM network is under pressure. Furthermore, the criticality index of the saturated elements indicate a magnitude of the improvement a rise in capacity of the element would bring to the objective function value. Having the information on the saturated sectors, and their criticality index, ANSPs could take mitigation actions to improve the situation on the day of operations. For example, a supervisor having one or two saturated sectors, both with the low criticality index, might decide that the planned configuration is good enough as even if the capacity ends up being violated it will be for a small number of flights, which in many cases is what already happens in every-day operations. However, if there are few sector-hours within an area control center with high criticality indexes, the supervisor might decide to change the configuration into a one that brings more capacity. Further, this change can be inserted into TW model to re-run it and check what impact it would have on this particular airspace, and the entire network.

In a different example, the TW model results could be used by the AUs. The AUs could inspect their constrained flights in terms of the flexibility assigned (i.e., low if they are constrained) and the saturation of the airspace the trajectory is planned to cross. For example, they could use the visualisation tool[4] for visual inspection. Through inspection they could decide to keep the constrained flight plan, or to file for re-route through less constrained airspace, if available. Even the decision of retaining the constrained flight plan can be of use to AUs as they would have early information on the flight that has to be operated with the particular precision. In the case the AU opts for the re-route, this information can also be re-run in the TW model to ascertain the impact on the individual flight and on the network as a whole.

To sum-up, the model results offer information on strategic flexibility and predictability, that can be used by different stakeholders, and the impact of the envisioned changes can be assessed. The next logical research step is to analyse in more detail the above described mitigation actions. For example, to identify saturated network elements, checking if configurations with higher capacity exist in that portion of airspace, and if they do, implement them in the TW model, and check for the overall impact.

8.2. Concluding remarks

In this paper, we describe three variations of the TW model, three types of TWs (forward, symmetric and asymmetric), and the computational experiments on real data with an entire day of traffic from the European ATM network. The three variants of the TW model give different results - the number of constrained flights per TW model variant is inversely proportional to the level of capacity utilisation and

[4] Available at https://visualization.adapt-h2020.eu/

therefore the conservative variant gives a greater number of constrained flights than the intermediate variant, which in turn has a larger number than the proportional one. In addition, the type of TW also impacts the number of constrained flights. In the three TW model variants, forward TWs always produce the lowest number of constrained flights when compared with the asymmetric (only conservative TW model) and symmetric TW type. Computational experiments show that on a busy day in the European network, with a particular (stringent) configuration in place, between 40 and 50 % of flights would be constrained (i.e., TWs lower than 15 min.), but not overly constrained (i.e., having TWs of 1 min.). Even though most of the flights do have some flexibility, this could be an indication of the insufficient capacity of the particular configurations in place at certain points in the network.

Global Air Navigation Plan (GANP) (ICAO, 2016) sets global performance ambitions, by defining 11 Key Performance Areas (KPAs), among them flexibility and predictability. Even though these two KPAs are recognised as important performance areas, common metrics are still not defined. Regarding the flexibility, GANP states "...the air navigation system should be flexible enough to integrate changes in business and operational trajectories at the frequency required by airspace users." Its relevance is therefore clearly stated, even though the metric to measure it is not defined. Predictability is another KPA widely recognised as important, as in order to provide as efficient service as possible, an entity should be able to accurately predict the future demands on its system. What is more important, all ATM stakeholders recognise the importance of both having the flexibility and providing predictability, but they are often seen as opposing - high predictability is considered to limit the flexibility in the system. We believe that the approach presented in this paper offers some insight in the requirements of information exchange needed to ensure a measure of predictability, and more importantly to attempt the quantification of flight flexibility. For predictability, different stakeholders have to exchange different types of information at certain time horizons. For example, the airspace configuration and capacities planned by ANSPs, and the set of routes acceptable by airlines between the origin and destination airports. When these are available strategically, a picture of constraints and saturation points in the network can be obtained, as well as the measure of flight flexibility. Having enough time prior to the day of operations, different settings can be tried out to help in making the final decision.

Of course, the strategic flight planning presented here is acceptable as long as these efforts result in better tactical/actual operations, where the goodness is measured in terms of delay and cost reduction, robustness of time windows, just to mention a few indicators. The first step in the robustness testing of TWs, presented in Section 7.3 shows that TWs could be used in operational strategic planning. With this result in mind, it is of great importance to assess the impact of strategic/pre-tactical planning on the tactical/actual operations. Thus, another line of future research direction lies in the assessment of the tactical impact of the strategic planning.

Acknowledgements

The work presented here is a result of the ADAPT project. This project has received funding from the SESAR Joint Undertaking under grant agreement No. 783264 under European Union's Horizon 2020 research and innovation programme. The opinions expressed herein reflect the author's view only. Under no circumstances shall the SESAR Joint Undertaking be responsible for any use that may be made of the information contained herein.

Glossary

References

Barnhart, C., Bertsimas, D., Caramanis, C., Fearing, D., 2012. Equitable and Efficient Coordination in Traffic Flow Management. Transportation Science 46, 262–280.

Barnhart, C., Cohn, A., Johnson, E., Klabjan, D., Nemhauser, G., Vance, P., 2003. Airline crew scheduling, in: Handbook of transportation science. Springer, pp. 517–560.

Berechet, I., Debouck, F., Castelli, L., Ranieri, A., Rihacek, C., 2009. A target windows model for managing 4-d trajectory-based operations. AIAA/IEEE Digital Avionics Systems Conference - Proceedings , 3.D.21–3.D.29.

Bertsimas, D., Lulli, G., Odoni, A., 2011. An integer optimization approach to large-scale air traffic flow management. Operations Research 59, 211–227.

Bertsimas, D., Stock Patterson, S., 1998. The air traffic flow management problem with enroute capacities. Operations Research 46, 406–422.

Bertsimas, D., Stock Patterson, S., 2000. The traffic flow management rerouting problem in air traffic control: A dynamic network flow approach. Transportation Science 34, 239–255.

Acronym	Definition
AIRAC	Aeronautical Information Regulation And Control
ANSP	air navigation service provider
ATC	air traffic control
ATFM	air traffic flow management
ATM	air traffic management
AU	airspace user
CRCO	Central Route Charging Office
DDR2	demand data repository 2
ECAC	European Civil Aviation Conference
GANP	Global Air Navigation Plan
KPA	key Performance Area
MTOW	maximum take-off weight
NOP	network operations plan
SATA	Strategic Air Traffic Assignment
TW	time window

Bolić, T., Castelli, L., Corolli, L., Rigonat, D., 2017. Reducing atfm delays through strategic flight planning. Transportation Research Part E 98, 42–59.

Bouras, A., Ghaleb, M., Suryahatmaja, U., Salem, A., 2014. The airport gate assignment problem: A survey. The Scientific World Journal 2014.

Brueckner, J., Czerny, A., Gaggero, A., 2021. Airline mitigation of propagated delays via schedule buffers: Theory and empirics. Transportation Research Part E: Logistics and Transportation Review 150, 102333.

Castelli, L., Corolli, L., Lulli, G., 2011. Critical flights detected with time windows. Transportation Research Record 2214, 103–110.

Chung, S.H., Ma, H.L., Hansen, M., Choi, T.M., 2020. Data science and analytics in aviation. Transportation Research Part E: Logistics and Transportation Review 134, 101837.

Cook, A.J., Tanner, G., 2015. European airline delay cost reference values. Technical Report. EUROCONTROL Performance Review Unit.

Corolli, L., Castelli, L., Lulli, G., 2010. The air traffic flow management problem with time windows, in: 4th International Conference on Research in Air Transportation (ICRAT), Budapest, Hungary, pp. 201–207.

Delgado, L., Gurtner, G., Bolić, T., Castelli, L., 2021. Estimating economic severity of air traffic flow management regulations. Transportation Research Part C: Emerging Technologies 125, 103054.

Ding, W., Zhang, Y., Hansen, M., 2018. Downstream impact of flight rerouting. Transportation Research Part C: Emerging Technologies 88, 176–186.

Estes, A.S., Ball, M.O., 2020. Equity and strength in stochastic integer programming models for the dynamic single airport ground-holding problem. Transportation Science 54, 944–955.

Eufrásio, A.B.R., Eller, R.A., Oliveira, A.V., 2021. Are on-time performance statistics worthless? An empirical study of the flight scheduling strategies of Brazilian airlines. Transportation Research Part E: Logistics and Transportation Review 145, 102186.

Eurocontrol, 2019a. CODA Digest 2019 - All-causes delay and cancellations to air transport in Europe. Technical Report. EUROCONTROL.

Eurocontrol, 2019b. Network Operations Report 2018. Technical Report. EUROCONTROL.

Güvercin, M., Ferhatosmanoglu, N., Gedik, B., 2020. Forecasting flight delays using clustered models based on airport networks. IEEE Transactions on Intelligent Transportation Systems 22, 3179–3189.

Han, F., Wong, W.B.L., Gaukrodger, S., 2010. Improving future air traffic punctuality:"pinch-and-pull" target windows. Aircraft Engineering and Aerospace Technology 82, 207–216.

ICAO, 2016. Global Air Navigation Plan, Doc 9750-AN/963, Fifth edition. Technical Report. International Civil Aviation Organization.

Ikli, S., Mancel, C., Mongeau, M., Olive, X., Rachelson, E., 2021. The aircraft runway scheduling problem: A survey. Computers & Operations Research 132, 105336.

Ivanov, N., Jovanović, R., Fichert, F., Strauss, A., Starita, S., Babić, O., Pavlović, G., 2019. Coordinated capacity and demand management in a redesigned air traffic management value-chain. Journal of Air Transport Management 75, 139 – 152.

Koksalmis, G., 2019. Operations management perspectives in the air transport management. Journal of Business Administration Research 2.

Kolidakis, S., Botzoris, G., 2018. Enhanced air traffic demand forecasting using artificial intelligence, in: The 6th Virtual Multidisciplinary Conference, pp. 126–131.

Liu, Y., Liu, Y., Hansen, M., Pozdnukhov, A., Zhang, D., 2019. Using machine learning to analyze air traffic management actions: Ground delay program case study. Transportation Research Part E: Logistics and Transportation Review 131, 80–95.

Lulli, G., Odoni, A., 2007. The european air traffic flow management problem. Transportation Science 41, 431–443.

Margellos, K., Lygeros, J., 2013. Toward 4-D Trajectory Management in Air Traffic Control: A Study Based on Monte Carlo Simulation and Reachability Analysis. IEEE Transactions on Control Systems Technology 21, 1820–1833.

Meyn, L., 2002. Probabilistic methods for air traffic demand forecasting, in: AIAA Guidance, Navigation, and Control Conference and Exhibit, p. 4766.

Mitici, M., Verbeek, R., van den Brandt, R., 2019. Advanced prediction models for flexible trajectory-based operations. Technical Report. Deliverable D4.1 of the Horizon 2020 ADAPT project.
Network Manager, 2018. IFPS users manual. EUROCONTROL.
Odoni, A.R., 1987. The flow management problem in air traffic control, in: Flow control of congested networks. Springer, pp. 269–288.
Olive, X., Basora, L., 2020. Detection and identification of significant events in historical aircraft trajectory data. Transportation Research Part C: Emerging Technologies 119, 102737.
Performance Review Commission, 2019. Performance Review Report 2019. Technical Report. EUROCONTROL.
Rodríguez-Sanz, Á., Comendador, F.G., Valdés, R.M.A., Pérez-Castán, J.A., García, P.G., Godoy, M.N.G.N., 2019. 4D-trajectory time windows: definition and uncertainty management. Aircraft Engineering and Aerospace Technology 91, 761–782.
Rodríguez-Sanz, Á., Puchol, C.C., Pérez-Castán, J.A., Comendador, F.G., Valdés, R.M.A., 2020. Practical implementation of 4D-trajectories in air traffic management: system requirements and time windows monitoring. Aircraft Engineering and Aerospace Technology 92, 1357–1375.
Sanjeevi, S., Venkatachalam, S., 2020. Robust flight schedules with stochastic programming. arXiv preprint arXiv:2001.08548 .
Shone, R., Glazebrook, K., Zografos, K.G., 2021. Applications of stochastic modeling in air traffic management: Methods, challenges and opportunities for solving air traffic problems under uncertainty. European Journal of Operational Research 292, 1–26.
Starita, S., Strauss, A.K., Fei, X., Jovanović, R., Ivanov, N., Pavlović, G., Fichert, F., 2020. Air Traffic Control Capacity Planning Under Demand and Capacity Provision Uncertainty. Transportation Science 54, 882–896.
Sun, X., Chung, S.H., Ma, H.L., 2020. Operational risk in airline crew scheduling: do features of flight delays matter? Decision Sciences 51, 1455–1489.
Vranas, P.B., Bertsimas, D., Odoni, A.R., 1994a. Dynamic ground-holding policies for a network of airports. Transportation Science 28, 275–291.
Vranas, P.B., Bertsimas, D., Odoni, A.R., 1994b. The multi-airport ground-holding problem in air traffic control. Operations Research 42, 249–261.
Wen, X., Ma, H.L., Chung, S.H., Khan, W., 2020. Robust airline crew scheduling with flight flying time variability. Transportation Research Part E: Logistics and Transportation Review 144, 102132.
Woo, Y.B., Moon, I., 2021. Scenario-based stochastic programming for an airline-driven flight rescheduling problem under ground delay programs. Transportation Research Part E: Logistics and Transportation Review 150, 102360.
Xu, Y., Dalmau, R., Melgosa, M., Montlaur, A., Prats, X., 2020. A framework for collaborative air traffic flow management minimizing costs for airspace users: Enabling trajectory options and flexible pre-tactical delay management. Transportation Research Part B: Methodological 134, 229 – 255.

Appendix A. Introducing capacity matters

European definition of a capacity is the number of entries within the defined time horizon, usually an hour. Thus, the nominal capacity defines how many flights can enter a sector during an hour, in nominal conditions. Unfavourable weather conditions, for instance, can require effective lowering of the nominal capacity, but that is done operationally, if there is a need for such measures (through ATFM measures).

Today, the airspace users do not need to consider the capacity of the airspace they would like to fly through. However, European ANSPs have the information on what is considered the nominal capacity of each of the sectors under their jurisdiction. The actual capacity of an ANSP at each point in time depends on the applied sectorisation (i.e., configuration). A particular configuration consists of a number of sectors. The higher the number of sectors in a configuration, the higher the capacity of the airspace under the configuration. Figure A.12 depicts two configurations of an ANSP: with just one sector (left figure), and with two sectors, where the division is in the horizontal plane (right figure). The nominal capacity of the first configuration is lower than that of the second one (42 compared to 95 entries in an hour).

The actual sectorisation is chosen by the supervisor, based on the traffic demand prediction (short-term prediction based on the submitted flight plans) and the staff availability. The changes are actuated when the need arises, at any time of day. As the configuration changes at need, the change can happen at any fraction of an hour. For example, it can happen that a particular configuration (see figure A.12a) is active from 8:00 to 10:20. In that case, the sector belonging to the configuration would have three sector-hour capacities assigned – two full sector-hour capacities (from 08:00 to 10:00) and a partial sector-hour capacity of 14 entries, the hourly capacity being scaled to 20 minutes. Two-sector configuration (figure A.12b) can be active from 10:20 to 11:00 where each sector of the configuration would have partial sector-hour capacities, with capacities scaled to 40 minutes of sector-hour duration. Thus, at each point in time, only the sectors belonging to the active configuration can be entered and crossed by flights.

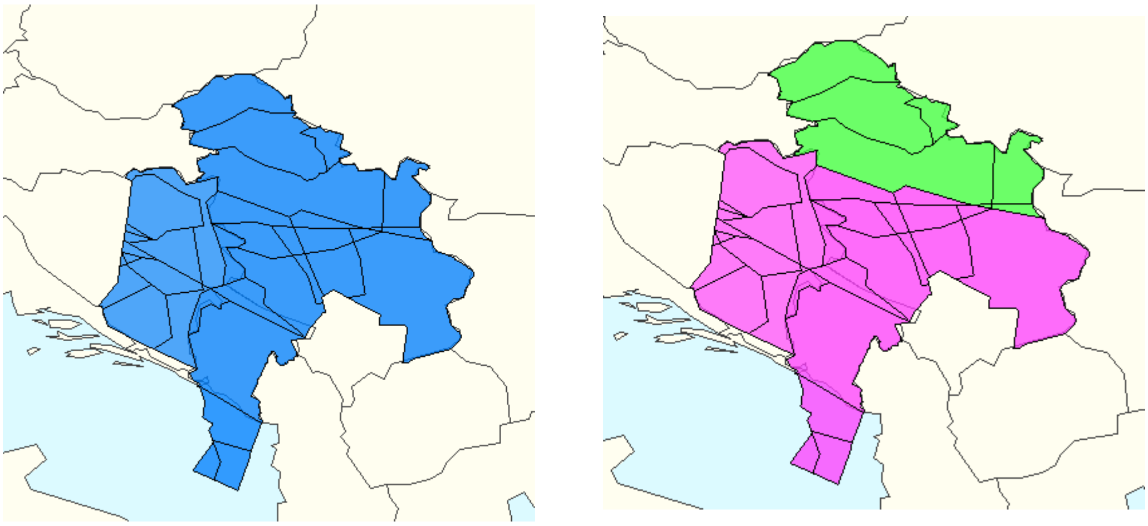

(a) One active sector *(b) Two active sectors*

Figure A.12: Sectorisation configurations with one active sector (left) and two active sectors (right).

Appendix B. Weight coefficients

Weight coefficients $\gamma(\tau)$ are introduced in the objective function (1) to favour TWs of similar duration to each of two flights, rather than the assignment of a large TW to one flight and a small one to another. This fairer distribution of TWs' duration is achieved by imposing that coefficients $\gamma(\tau)$ decrease as $|\tau|$ grows, so that greater weights are given to time periods closer to the assigned departure time d_f, where $\gamma(\tau)$ is the weight associated with the period t such that $t - d_f = \tau$.

Since the objective to be guaranteed is in any case the maximisation of flexibility, and therefore of the overall duration of the TW, in the following we define a sequence of decreasing weights which, within the same maximum duration of TWs, allows a more equitable distribution of TWs among the various flights.

If we set $w_m = max(w^-_{max}, w^+_{max} - 1)$, the coefficients could therefore be defined as:

$$\gamma(\tau) = 1 - \frac{|\tau|}{x} \text{ where } -w^-_{max} \leq \tau \leq w^+_{max} - 1 \text{ and } x > w_m. \tag{B.1}$$

Thus,

$$1 = \gamma(0) > \gamma_{max} = \gamma(\pm 1) > \cdots > \gamma(\pm w_m) = \gamma_{min}$$

Weight $\gamma(0)$, associated with the assigned departure time d_f, is equal to 1; γ_{max} is the weight associated with the time periods adjacent to d_f and, except for $\gamma(0)$, is the maximum weight; γ_{min} is associated with the most distant time periods from d_f.

If we consider a feasible solution n for the TW optimisation problem (constraints (2) - (13)), we define $\mathcal{D}^n$ as the total sum of the number of time periods in which TWs are open, i.e., the total TW duration,

$$\mathcal{D}^n = \sum_{f \in \mathcal{F}, t \in \mathcal{T}_{f,1}} x^n_f(t),$$

and $\mathcal{O}^n$ as the value of the objective function (1) for n, i.e., the weighted total TW duration,

$$\mathcal{O}^n = \sum_{f \in \mathcal{F}, t \in \mathcal{T}_{f,1}} x^n_f(t) \cdot \gamma(t - d_f).$$

$\mathcal{D}^n$ would be equal to $\mathcal{O}^n$ if the weight coefficients γ all had value 1.

Our goal is to choose values for the coefficients γ such that, given two feasible solutions n_1 and n_2, it is always true that

a) Any preferable feasible solution in terms of the objective function (1), must have a greater total TWs duration, i.e.,

$$\mathcal{O}^{n_1} > \mathcal{O}^{n_2} \Rightarrow \mathcal{D}^{n_1} \geq \mathcal{D}^{n_2}; \tag{B.2}$$

b) A solution with a greater duration also implies that it is preferable in terms of the weighted duration, i.e., of the objective function (1:)

$$\mathcal{D}^{n_1} > \mathcal{D}^{n_2} \Rightarrow \mathcal{O}^{n_1} > \mathcal{O}^{n_2} \tag{B.3}$$

In such a way if two solutions have the same total duration, the preferable solution is the one with a more equitable distribution of TWs' duration. Therefore the optimal solution $\mathcal{O}$ must also have the maximum value of $\mathcal{D}$.

As an example, let n_1 and n_2 be two feasible solutions which differ only in the three TWs, tw_a, tw_b and tw_c, as shown in figure B.13.

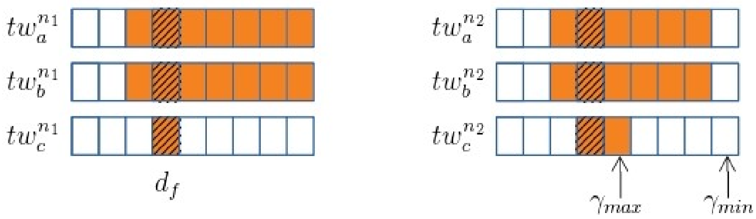

Figure B.13: Two feasible solutions n_1 and n_2, which differ only in the three TWs. $D^{n_1} = 15$ and $D^{n_2} = 14$, hence n_1 is a preferable solution with respect to n_2.

n_1 is a preferable solution with respect to n_2 because $\mathcal{D}^{n_1} = \mathcal{D}^{n_2} + 1$. In order for equation B.3 to be valid, or rather $\mathcal{O}^{n_1} > \mathcal{O}^{n_2}$, it is necessary that $2\gamma_{min} > \gamma_{max}$. In fact, $n1$ has tw_a and tw_b open in the time periods furthest from the start (those associated with the minimum weight) while in $n2$ they are closed. $n2$ has tw_c open in the time period closest to the start (associated with the maximum weight) while in $n1$ this is closed. Since these are the only differences, in order for $n1$ to be preferable to $n2$ (i.e., in order to have $\mathcal{O}^{n_1} > \mathcal{O}^{n_2}$), it is necessary that 2 times the minimum weight be greater than the maximum weight. If this inequality is valid, also $2\gamma^{'} > \gamma^{''}$ is valid for any pair of cost coefficients $\gamma^{'}$ and $\gamma^{''}$ such that $\gamma_{min} \leq \gamma^{'} < \gamma^{''} \leq \gamma_{max}$.

More generally, the inequality should be valid for any number m of time periods with the minimum weight that must have a total weight greater than $m-1$ periods with the maximum weight. To guarantee this, a characteristic that the weight coefficients γ must have is the following:

$$m\gamma_{min} > (m-1)\gamma_{max} \text{ where } m \text{ is such that } 2m-1 \leq |\mathcal{F}|.$$

Considering that the maximum value for m is $\frac{|\mathcal{F}|+1}{2}$ and the fact that the total number of flights is $|\mathcal{F}|$, we must make sure that:

$$\gamma_{min} > \frac{|\mathcal{F}|-1}{|\mathcal{F}|+1}\gamma_{max} \tag{B.4}$$

Combining equations B.1 and B.4 together:

$$\begin{aligned} 1 - \frac{w_m}{x} &> \frac{|\mathcal{F}|-1}{|\mathcal{F}|+1}(1 - \frac{1}{x}) \\ (|\mathcal{F}|+1)(x - w_m) &> (|\mathcal{F}|-1)(x-1) \\ x &> \frac{|\mathcal{F}|(w_m - 1) + w_n + 1}{2} \end{aligned} \tag{B.5}$$

Then we can set $x = \frac{|\mathcal{F}|}{2} w_m$ and therefore define the weight coefficients γ as:

$$\gamma(\tau) = 1 - \frac{2|\tau|}{w_m \cdot |F|} \qquad - w_{max}^{-} \leq \tau \leq w_{max}^{+} - 1$$

Appendix C. Capacity utilisation coefficient

When a TW is completely contained within a single sector-hour, it uses a unit of capacity. If, on the other hand, it spans two sectors-hours, in the conservative case a unit of capacity is reserved in both sectors, thus resulting in its under-utilisation since a flight will actually enter one or the other of the two sectors-hours. For this reason, the proportional and intermediate variants have been introduced (Section 4) and the amount of capacity that must be reserved for that flight changes.

To compute the exact sector-hour utilisation value, a *capacity utilisation coefficient* β is introduced. In case a TW extends over two sector-hours, one of the two contains the assigned time of entry $d_f + l^i_{r_f}$, while the other only intersects either $\mathcal{T}^+_{f,i}$ or $\mathcal{T}^-_{f,i}$. For simplicity, we denote the latter sector-hour as c^*. Both in proportional and intermediate variants a fraction q^* of unit of capacity of c^* equal to the fraction of time periods of the TW present in sector-hour c^* is reserved. In the former sector-hour, a whole unit of capacity is reserved in the intermediate variant, while a fraction of unit of capacity equal to $1 - q^*$ is reserved in the proportional variant. Therefore, to define the variants of the TW model it is sufficient to define only the *capacity utilisation coefficients* β^i_{f,c^*} relating to sector-hours c^* which do not contain the time assigned for the i-th operation of flight f. We define these coefficients coefficients as B.

Coefficient B can be defined as $B(\delta, \tau)$ ($\in [0, 1]$), where δ and τ are such that:

- δ is the time difference between the assigned time of entry $d_f + l^i_{r_f}$ and the first period, closest to $d_f + l^i_{r_f}$, in which flight f may reserve capacity in sector-hour c^*.
  - When c^* intersects $\mathcal{T}^+_{f,i}$, as in upper case shown in Fig.C.14 (for which $c^* = c_2$), $\delta = open_{c^*} - d_f + l^i_{r_f}$.
  - When c^* intersects $\mathcal{T}^-_{f,i}$, as in lower case shown in Fig.C.14 (for which $c^* = c_1$), $\delta = d_f + l^i_{r_f} - close_{c^*} + 1$.

  where $open_c$ and $close_c$ represent the opening and closing time periods of sector-hour c, respectively.
- τ is the difference between each of the TW periods covered by c^* and the assigned time of entry $d_f + l^i_{r_f}$.

We notice however that we can apply the intermediate and proportional TW model variants only for *forward* or *symmetric* TW types, because only in these cases we are able to implement the coefficient B.

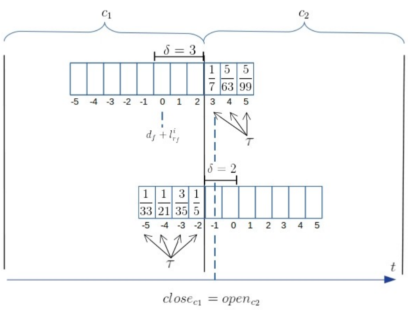

Figure C.14: Two TWs that extend over sector-hours c_1 e c_2 for the Symmetric type.

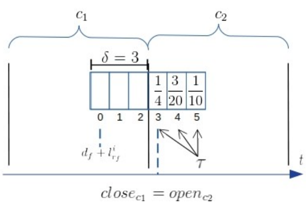

Figure C.15: A TW that extends over sector-hours c_1 e c_2 for the Forward type.

In fact, in both *forward* and in *symmetric TW* types, in case a TW extends over two sector-hours, it is sufficient to know the value of the decision variables for the TW periods covered by c^* to establish the fractions of unit of capacity to be reserved in each of the two sector-hours.

Forward TWs. In this case, a TW can only extend forward with respect to the assigned time of entry $d_f + l^i_{r_f}$, i.e., $w^-_{max} = 0$, $T^-_{f,i} = \emptyset$, therefore for the monotony constraint (2), if the TW is open in the period $d_f + l^i_{r_f} + \tau$, then the duration of the TW is at least $\tau + 1$.

As an example, the TW depicted in Figure C.15 starts in c_1, 3 minutes before the activation of the hour sector c_2 ($\delta = 3$). If the TW were not open 3 minutes after the time assigned by the SATA, that is in the first instant of activation of c_2, then it would not be necessary to reserve any capacity in c_2.

Table C.7: $B(\delta,\tau)$ coefficients for Forward TWs with $w^-_{max}=0$ and $w^+_{max}=5$

	$\tau=1$	$\tau=2$	$\tau=3$	$\tau=4$
$\delta=1$	$\frac{1}{2}$	$\frac{1}{6}$	$\frac{1}{12}$	$\frac{1}{20}$
$\delta=2$		$\frac{1}{3}$	$\frac{1}{6}$	$\frac{1}{10}$
$\delta=3$			$\frac{1}{4}$	$\frac{3}{20}$
$\delta=4$				$\frac{1}{5}$

Table C.8: $B(\delta,\tau)$ coefficients for Symmetric TWs with $w^-_{max}=4$ and $w^+_{max}=5$

	$\lvert\tau\rvert=1$	$\lvert\tau\rvert=2$	$\lvert\tau\rvert=3$	$\lvert\tau\rvert=4$
$\delta=1$	$\frac{1}{3}$	$\frac{1}{15}$	$\frac{1}{35}$	$\frac{1}{63}$
$\delta=2$		$\frac{1}{5}$	$\frac{3}{35}$	$\frac{1}{21}$
$\delta=3$			$\frac{1}{7}$	$\frac{5}{63}$
$\delta=4$				$\frac{1}{9}$

If instead it were open at the time period $d_f + l^i_{r_f} + 3$ ($\tau = 3$) then it would reserve in c_2 a fraction of capacity equal to $\frac{1}{4}$, since it would have a duration of 4 time periods, of which 1 in c_2, otherwise no capacity would be reserved. If the TW would be open at the time period $d_f + l^i_{r_f} + 4$ ($\tau = 4$) then a total of $\frac{2}{5}$ of a capacity unit would be reserved, since it would have a duration of 5 time periods, of which 2 in c_2. Having already reserved 1/4 unit of capacity, to obtain 2/5 it is sufficient to add 3/20, and so on.

The fraction of capacity to be reserved can therefore be obtained as the sum of the coefficients $B(\delta,\tau)$ through which a weight is given to each time period in which TW is open. In this way, the capacity q_{c_2} to be reserved in c_2 is calculated, while for the sector-hour c_1 a whole unit of capacity will be reserved in the intermediate TW model variant, or $1 - q_{c_2}$ of unit of capacity in the case of proportional model variant.

Symmetric TWs. Similar considerations can be made in this case, taking into account that, exploiting symmetry and monotony constraints (6, 2 and 3), the TW is open at time period $d_f + l^i_{r_f} + \tau$, if it is open at $d_f + l^i_{r_f} - \tau$ and vice-versa. Therefore if the TW is open in the period $d_f + l^i_{r_f} + \tau$, the duration of the TW is at least $2\tau + 1$, and the fractions of units of capacity to be reserved change accordingly.

Asymmetric TWs. In thic case, instead, if the TW were open 3 minutes after the instant assigned by the SATA, we cannot know before solving the optimisation problem what fraction of capacity to reserve in c_2 precisely because we cannot know how long the TW has extended.

More generally, coefficients $B(\delta,\tau)$, $\tau \geq \delta$ are defined as follows:

$$B(\delta,\tau) = \begin{cases} \frac{\delta}{|\tau|(|\tau|+1)} & \text{Forward Model} \\ \frac{2\delta-1}{(2|\tau|-1)(2|\tau|+1)} & \text{Symmetric Model} \end{cases}$$
$$\forall\delta \in [1; max(w^-_{max}, w^+_{max}-1)], \forall\tau \in [-w^-_{max}; w^+_{max}-1)], |\tau| \geq \delta$$

Tables C.7 and C.8 give an example of the $B(\delta,\tau)$ coefficients for *forward* and *symmetric* TWs.

Once coefficients $B(\delta,\tau)$ are defined, it is possible to formulate the capacity counts (14), (15), and (16) for both the intermediate and the proportional variant. Here we show how to derive equation (16) in the symmetric case. The others cases follow similar arguments.

As in the symmetric case TWs extend backward and forward with respect to the assigned time of entry into a sector-hour, in figure C.16 we depict five different cases of positioning of TWs within a sector-hour. For flights f, $d_f + l^i_{r_f}$ is the time period in which the i-th action is assigned, and is represented by the shaded rectangles in the figure. $\mathcal{T}^-_{f,i}$ is the set of time periods within which the sector entry can be performed earlier than assigned, and $\mathcal{T}^+_{f,i}$ is the set of time periods in which the sector entry can be on time or postponed.

In Figure C.16 we can see two TWs with $d_f + l^i_{r_f} \notin \mathcal{T}^c$ (cases 1 and 5): in these two cases, for both model variants a fraction calculated as the sum of the coefficients $B(\delta,\tau)$ for the time periods in which the TW is open will be reserved in c. For TWs with $d_f + l^i_{r_f} \in \mathcal{T}^c$ (cases 2, 3 e 4), in the intermediate variant, a whole unit of capacity in c will be reserved. Conversely, in the proportional variant, only for case 3 a whole unit of capacity will be reserved in c; in cases 2 and 4 a fraction of the unit of capacity corresponding to the quantity reserved by the same TW in the adjacent sector-hour must be discounted.

Thus, for the intermediate variant, the number of entries in sector-hour c of sector j (Equation 16) becomes:

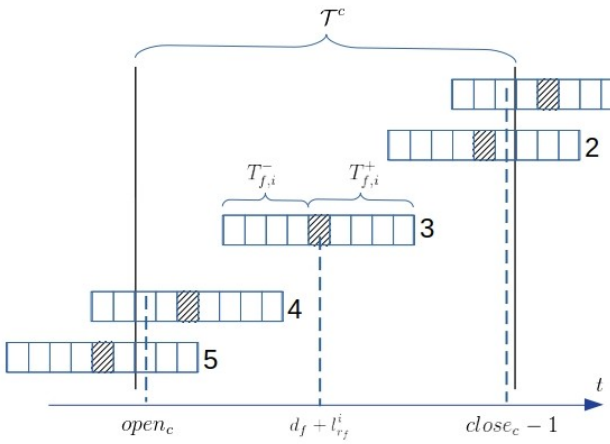

Figure C.16: All five different cases of positioning of TWs within a sector-hour c.

$$
\begin{aligned}
ent^{int}_{j,c} :=& \sum_{\substack{f\in\mathcal{F}, i\in[2,n_f-1], t\in\mathcal{T}^c:\\ t=d_f+l^i_{r_f}\wedge s^i_{r_f}=j}} x_f(t-l^i_{r_f}) \\
&+ \sum_{\substack{f\in\mathcal{F}, i\in[2,n_f-1], t\in\mathcal{T}^c\cap\mathcal{T}^+_{f,i}:\\ d_f+l^i_{r_f}<open_c\wedge s^i_{r_f}=j}} B(open_c-(d_f+l^i_{r_f}), t-(d_f+l^i_{r_f}))\cdot x_f(t-l^i_{r_f}) \\
&+ \sum_{\substack{f\in\mathcal{F}, i\in[2,n_f-1], t\in\mathcal{T}^-_{f,i}:\\ d_f+l^i_{r_f}\geq close_c\wedge s^i_{r_f}=j}} B((d_f+l^i_{r_f})-close_c+1, t-(d_f+l^i_{r_f}))\cdot x_f(t-l^i_{r_f})
\end{aligned}
\tag{C.1}
$$

Instead, for the proportional variant, equation (16) becomes:

$$
\begin{aligned}
ent^{prop}_{j,c} :=& ent^{int}_{j,c} \\
&- \sum_{\substack{f\in\mathcal{F}, i\in[2,n_f-1], t\in\mathcal{T}^+_{f,i}:\\ d_f+l^i_{r_f}<close_c\wedge t\geq close_c\wedge s^i_{r_f}=j}} B(close_c-(d_f+l^i_{r_f}), t-(d_f+l^i_{r_f}))\cdot x_f(t-l^i_{r_f}) \\
&- \sum_{\substack{f\in\mathcal{F}, i\in[2,n_f-1], t\in\mathcal{T}^-_{f,i}:\\ d_f+l^i_{r_f}\geq open_c\wedge t<open_c\wedge s^i_{r_f}=j}} B((d_f+l^i_{r_f})-open_c+1, t-(d_f+l^i_{r_f}))\cdot x_f(t-l^i_{r_f})
\end{aligned}
\tag{C.2}
$$

Capacity counts (14) and (15) are implemented in a similar way.

Appendix D. TW Robusteness model

This model appropriately modifies the TW model presented in Section 3. Its aim is to minimise the TW violations, as introduced in Section 7.3, to evaluate the effects of not respecting the departure TW by a set $\mathcal{D} \subseteq \mathcal{F}$ of flights.

Appendix D.1. Notation

Appendix D.1.1. Sets

$\mathcal{A} \equiv$ set of airports, indexed by a
$\mathcal{S} \equiv$ set of sectors, indexed by s
$\mathcal{F} \equiv$ set of flights, indexed by f
$\mathcal{D} \equiv$ set of delayed flights that are assigned a delayed departure time d_f^D
$\mathcal{G} \equiv$ set of pairs of flights (f', f'') that are connected, with turnaround time $g_{f',f''}$
$\mathcal{R} \equiv$ set of routes, indexed by r, where r_f is the chosen route for flight f
$\mathcal{B} \equiv \{dep, arr, gen, ent\} \equiv$ set of operations that can be performed by a flight, where arr, dep, and gen stand for arrival, departure or generic movement type (can be arrival or departure) at an airport, and ent stands for entry into a sector
$\mathcal{C}_j^b \equiv$ set of sector-hours linked with the operation b at sector or airport j, indexed by c
$\mathcal{T}^c \equiv$ set of time periods during which sector-hour c is active

Appendix D.1.2. Parameters

$orig_f \equiv$ departure airport of flight f
$dest_f \equiv$ destination airport of flight f
$n_f \equiv$ number of elements (sectors and airports) along the chosen route r_f
$s_r^i \equiv$ i-th element of route r
$l_r^i \equiv$ flight time from origin to the i-th element of route r
$tw_f^{start} \equiv$ first time of the departure TW of flight f
$tw_f^{end} \equiv$ last time of the departure TW of flight f
$d_f^D \equiv$ delayed departure time of flight f
$g_{f',f''} \equiv$ turnaround time between incoming flight f' and outgoing flight f", performed by the same aircraft
$open_c \equiv$ opening time period for sector-hour c (i.e., opening time of sector-hour c)
$close_c \equiv$ closing time period for sector-hour c
$\mathcal{Q}_c \equiv$ capacity enforced during sector-hour c, (i.e., declared capacity of a sector j, during the sector-hour c)

Appendix D.1.3. Parameter-depending sets

$$\mathcal{T}_{f,i} \equiv \{tw_f^{start} + l_{r_f}^i, \ldots, tw_f^{end} + l_{r_f}^i + 60\}$$
$\equiv$ set of feasible updated time periods for flight f to arrive at i-th element of its route r_f

Appendix D.2. Decision variables

Decision variables $x_f(t)$ are used to model the updated departure time d_f^U for flight f, v_f is its TW violation.

$$x_f(t) = \begin{cases} 1 & \text{if } t \text{ is the updated departure time of flight } f \\ 0 & \text{otherwise} \end{cases} \qquad \forall f \in \mathcal{F}, t \in \mathcal{T}_{f,1}$$

$$d_f^U = \sum_{t \in \mathcal{T}_{f,1}} x_f(t) \cdot t \qquad \forall f \in \mathcal{F} \tag{D.1}$$

$$v_f = \begin{cases} d_f^U - tw_f^{end} & \text{if } d_f^U > tw_f^{end} \quad (f \text{ is not able to meet its TW }) \\ 0 & \text{otherwise} \end{cases} \qquad \forall f \in \mathcal{F}, t \in \mathcal{T}_{f,1}$$

Appendix D.3. Objective function

The objective function minimises the total TW violation.

$$min \sum_{f \in \mathcal{F}} v_f \tag{D.2}$$

Appendix D.4. Constraints

Appendix D.4.1. TW violation definition

If a flight is able to execute the departure within its TW, it has a null TW violation, otherwise TW violation is equal to the difference between the updated departure time d_f^U and the end of the TW tw_f^{end}.

$$v_f(t) \geq 0 \qquad \forall f \in \mathcal{F} \tag{D.3}$$

$$d_f^U - tw_f^{end} \leq v_f \qquad \forall f \in \mathcal{F} \tag{D.4}$$

Since we propose the minimisation of violations v_f can only be either 0 or $d_f^U - tw_f^{end}$ depending on whether the flight is able to depart within its TW or not.

Appendix D.4.2. Updated departure time constrained

All flights are assigned a single updated departure time d_f^U; all delayed flights $f \in \mathcal{D}$ must be assigned an updated departure time d_f^U equal to or later than the delayed departure time d_f^D.

$$\sum_{t \in \mathcal{T}_{f,1}} x_f(t) = 1 \qquad \forall f \in \mathcal{F} \tag{D.5}$$

$$d_f^U \geq d_f^D \qquad \forall f \in \mathcal{D} \tag{D.6}$$

Appendix D.4.3. Connectivity constraints

Connectivity constraints guarantee that the time between the arrival of the incoming flight f' and the departure of the outgoing flight f'', performed by the same aircraft, is greater or equal to the turnaround time $g_{f',f''}$:

$$x_{f'}(t') + x_{f''}(t'') \leq 1 \qquad \forall (f', f'') \in \mathcal{G}, t' \in \mathcal{T}_{f',1}, t'' \in T_{f'',1} \colon t' + l_{r_{f'}}^{n_{f'}} + g_{f',f''} \geq t'' \tag{D.7}$$

Appendix D.4.4. Capacity constraints

The number of departures dep_c^a and arrivals arr_c^a at an airport a during the sector-hour c, are calculated as follows:

$$dep_c^a := \sum_{f \in \mathcal{F}, t \in \mathcal{T}^c \cap \mathcal{T}_{f,1} \colon orig_f = a} x_f(t) \tag{D.8}$$

$$arr_c^a := \sum_{f \in \mathcal{F}, t \in \mathcal{T}^c \cap \mathcal{T}_{f,n_f} \colon dest_f = a} x_f(t - l_{r_f}^{n_f}) \tag{D.9}$$

Further, the number of entries ent_c^j in the sector-hour c, of a sector j is calculated as follows:

$$ent_c^j := \sum_{f \in \mathcal{F}, i \in [2, n_f - 1], t \in \mathcal{T}^c \cap \mathcal{T}_{f,i} \colon s_{r_f}^i = j} x_f(t - l_{r_f}^i), \tag{D.10}$$

Thus, the capacity constraints can be expressed as:

$$dep_c^a \leq \mathcal{Q}_c \qquad \forall a \in \mathcal{A}, c \in \mathcal{C}_a^{dep} \tag{D.11}$$

$$arr_c^a \leq \mathcal{Q}_c \qquad \forall a \in \mathcal{A}, c \in \mathcal{C}_a^{arr} \tag{D.12}$$

$$dep_c^a + arr_c^a \leq \mathcal{Q}_c \qquad \forall a \in \mathcal{A}, c \in \mathcal{C}_a^{gen} \tag{D.13}$$

$$ent_c^j \leq \mathcal{Q}_c \qquad \forall j \in \mathcal{S}, c \in \mathcal{C}_j^{ent} \tag{D.14}$$